LAWRENCE
LIVERMORE
NATIONAL
LABORATORY

LLNL-JRNL-414524

On the Low Pressure Shock Initiation of Octahydro-1,3,5,7-Tetranitro-1,3,5,7-Tetrazoci (HMX) Based Plastic Bonded Explosives

K. S. Vandersall, C. M. Tarver, F. Garcia, S. K. Chidester

July 9, 2009

Journal of Applied Physics

Disclaimer

ON THE LOW PRESSURE SHOCK INITIATION OF OCTAHYDRO-1,3,5,7–TETRANITRO-1,3,5,7-TETRAZOCINE (HMX) BASED PLASTIC BONDED EXPLOSIVES

Kevin S. Vandersall, Craig M. Tarver, Frank Garcia, and Steven K. Chidester

Energetic Materials Center, Lawrence Livermore National Laboratory, Livermore, CA 94551

ABSTRACT: In large explosive and propellant charges, relatively low shock pressures on the order of 1 – 2 GPa impacting large volumes and lasting tens of microseconds can cause shock initiation of detonation. The pressure buildup process requires several centimeters of shock propagation before the transition to detonation occurs. Normally shock to detonation transition (SDT) is studied using shock pressures greater than 2.5 GPa that cause run distances to detonation of less than 3 cm. This paper presents experimentally measured longer run distance to detonation versus lower input shock pressure (often called "Pop Plot") data and embedded manganin gauge pressure histories for six octahydro-1,3,5,7–tetranitro-1,3,5,7-tetrazocine (HMX) based plastic bonded explosives. The six HMX PBX's studied are: PBX 9404; LX-04; LX-07; LX-10; PBX 9501; and EDC37. This data was obtained using 90 mm and 145 mm diameter cylindrical explosive charges impacted by projectiles accelerated by 101 mm and 155 mm diameter guns, respectively. The experimental data is analyzed using the Ignition and Growth reactive flow model of shock initiation and detonation for solid explosives. Existing higher shock pressure Ignition and Growth models for the six explosives are extended to include the lower shock pressure results. These reactive flow models can then be used to predict shock initiation or failure in large charges for hazard and accident scenarios that cannot be tested directly.

INTRODUCTION

The most frequent method of presenting shock initiation data for solid explosives and propellants is to measure the run distances to detonation for several input shock pressures and then plot the data on log-log axes. This graphical representation is called the "Pop Plot," named after Anthony Popolato of Los Alamos National Laboratory. Pop Plots first appeared in the shock initiation study of several explosives

by Ramsay and Popolato.[1] These plots give a clear indication of the relative shock sensitivities of different materials and the lengths of explosive charges needed for shock to detonation transition (SDT) to occur for one-dimensional sustained shock pressures. Over the middle of the shock initiation pressure range (2.5 GPa to 20 GPa for HMX based PBX's), linear fits accurately describe Pop Plot data. Figure 1 contains linear fits for the six HMX based PBX's discussed in this paper.[2] However, at the very high pressures produced by detonators and booster charges, the times and run distances to detonation are much shorter than those predicted by the linear fits. At lower shock pressures, the times and run distances are much longer than predicted by extension of the linear fit. For each explosive charge length, at some shock pressure SDT cannot occur. Low shock pressures are representative of many safety and vulnerability scenarios in which large, relatively slow fragments impact large areas of bare or covered explosive charges. This low shock pressure regime of SDT has not frequently been studied quantitatively, because of difficulties in handling large HMX charges and in producing sustained one-dimensional shock waves over large volumes. Several qualitative two-dimensional tests, such as confined and unconfined gap tests, have been used instead.[2]

To understand shock initiation and develop predictive reactive flow models, the most important experimental SDT data sets are the pressure and/or particle velocity histories measured by gauges embedded within the explosive charge. Manganin piezoelectric gauges are used to measure the pressure buildup caused by exothermic reaction behind the leading shock front at several positions within the explosive charge.[3] Metal particle velocity gauges[4] embedded in an explosive charge placed within a strong magnetic field yield the particle velocity build up rates at several positions within the reacting explosives. The two gauge techniques have been shown to yield equivalent results through the use of the Ignition and Growth hydrodynamic reactive flow model.[5] In the experimental portion of this study, manganin pressure gauges are embedded in 90 mm diameter by up to 405mm long and 145 mm diameter by 80 mm long cylinders of HMX PBX and impacted by flyer plates accelerated by a 101 mm powder gun or a 155 mm Howitzer gun, respectively, at various impact velocities to produce several different run distances to detonation. New and previously reported data are complied to show the relative shock sensitivity of 6 HMX PBX's at low shock pressures. The 6 PBX's are: PBX 9404 (94% HMX, 3% nitrocellulose, 3% chloroethylphosphate[CEF]); LX-04 (85% HMX; 15% Viton); LX-07 (90% HMX, 10%

Viton); LX-10 (95% HMX, 5% Viton); PBX 9501 (95% HMX, 2.5% BDNPA/F, 2.5% Estane); and EDC 37 (91% HMX, 9% nitrocellulose/K10 binder). In the reactive flow modeling portion of this study, the measured pressure histories and run distances to detonation are used to modify existing higher shock pressure Ignition and Growth model parameters for these 6 PBX's to account for this lower shock pressure data.

EXPERIMENTAL

In this experimental study, embedded manganin pressure gauges are placed along the axis of HMX PBX charges, which are impacted by flyer plates accelerated by two guns. For higher pressure and shorter run distances to detonation, a 101 mm powder gun accelerates 25 mm long by 101 mm diameter flyer plates into explosive targets that are 90 mm diameter by up to 45 mm long. Various thicknesses of the 90 mm diameter PBX discs are used to measure pressure histories at various distances into the PBX. To study lower shock pressures and longer run distances, a 155 mm Howitzer gun accelerates 50 mm long by 155 mm diameter metal plates into 145 mm diameter by 80 mm long explosive targets. In these targets, the manganin gauges are placed 10 mm apart on the charge axis of the target PBX cylinder. Two manganin gauges are placed in each gauge layer to provide redundancy. The manganin gauge records are only reliable when the flow is one-dimensional, because their electrical signals are not calibrated when they are stretched by lateral rarefaction waves. Two-dimensional Ignition and Growth calculations are used to determine where and when this stretching occurs.

This paper summarizes all of the work done on the six HMX PBX's at lower shock pressures. Previously reported run distances to detonation are included for completeness, but only previously unreported manganin gauge records and Ignition and Growth calculations are shown in detail. For PBX 9404, the oldest and most sensitive HMX PBX due to the sensitive nitrocellulose component in its binder, only 3 Howitzer experiments reported by Green et al.[6] in 1978 exist. The manganin gauges and reactive flow modeling were still in development at that time so they must be considered qualitative, but the run distances at three shock pressures are correct. A very comprehensive Ignition and Growth model for PBX 9404 was later developed that calculated these run distances to detonation accurately.[7] All of the LX-04 experimental and modeling results were recently published by Vandersall et al.[8] Some of the PBX 9501[9] and LX-10[10] experimental and modeling results were previously published, but all of the LX-07 and EDC

37 results are new. Table 1 lists the details of the new experiments for LX-10, PBX 9501, LX-07, and EDC37. The shot numbers for the 101 mm gun experiments in Table 1 begin with 47, while the 155 mm Howitzer gun shot numbers begin with HG. The impact velocities, flyer and impact plate material, approximate input pressure, and measured run distance to detonation are also listed in Table 1. The individual manganin gauge records and run distances to detonation for all of these experiments are shown in the Results section.

IGNITION AND GROWTH MODEL

The Ignition and Growth reactive flow model of shock initiation and detonation has been used to understand for many shock initiation and detonation studies of solid explosives and propellants in several 1D, 2D, and 3D codes.[11-15] The model uses two Jones-Wilkins-Lee (JWL) equations of state, one for the unreacted explosive and one for its reaction products, in the temperature dependent form:

$$p = Ae^{-R1V} + Be^{-R2V} + \omega C_v T/V \qquad (1)$$

where p is pressure in megabars, V is relative volume, T is temperature, ω is the usual Gruneisen coefficient, C_V is the average heat capacity, and A, B, R_1, and R_2 are constants. The reaction rate law for the conversion of explosive to products is:

$$dF/dt = \underset{0<F<F_{igmax}}{I(1-F)^b(\rho/\rho_o - 1 - a)^x} + \underset{0<F<F_{G1max}}{G_1(1-F)^cF^dp^y} + \underset{F_{G2min}<F<1}{G_2(1-F)^eF^gp^z} \qquad (2)$$

Ignition Growth Coalescence

where F is the fraction reacted, t is time, ρ is the current density, ρ_o is the initial density, and I, G_1, G_2, a, b, c, d, e, g, x, y, and z are constants. The mixture equations assume pressure and temperature equilibration between the unreacted explosive and its reaction products.

The unreacted JWL for any explosive is fit to experimental shock compression data and nanosecond time resolved von Neumann spike data for the detonating explosive.[16] The reaction product JWL equation of state is fit to the wall velocity expansion data from cylinder tests and laser interferometric interface velocity data for steady[17,18] and overdriven detonations.[19] The three-term rate law describes the three stages of reaction generally observed in shock initiation and detonation of heterogeneous solid explosives. For solid explosive shock initiation modeling, the first term of Equation (2) represents the

ignition of the explosive as it is compressed by the leading shock wave creating "hot spots" that can react and grow or fail to grow.[20] The fraction of explosive ignited is assumed to be equal to the void volume of the pressed explosive and is reacted in nanoseconds. For most of these PBX's, the initial void volume is about 2%. The second reaction rate in Eq. (4) models the relatively slow growth of the reacting "hot spots" as they consume the neighboring shock heated material. The third term in Eq. (4) describes the relatively fast process of coalescence of the growing hot spots and the rapid transition to detonation that consumes any remaining unreacted explosive.

In most previous HMX PBX modeling studies, the critical compression required for ignition [parameter a in the first term of Eq. (2)] was set equal to zero, because HMX explosives have been shown to react violently at low input pressures as low as 0.1 GPa in impact experiments involving friction and shear.[21] However, for pure shock compression at low pressure, the strength of the PBX limits the work done during void collapse, and a critical pressure for shock initiation is observed. In this modeling study, a critical compression value is found for each of the HMX PBX's to account for this effect. Since a critical compression value for ignition mainly affects the Ignition term of Eq. (2), which reacts at most 2% of the explosive, the use of this term has little or no effect on the growth and coalescence reaction rates. Thus the previous higher shock pressure modeling results are not affected. The entire experimental geometry is modeled, including each 0.3 mm thick manganin gauge package, in which the manganin foil is coated front and rear with about 125 μm of Teflon. To compare calculated pressure histories with the manganin gauge records, the middle zone of each 0.3 mm thick Teflon layer is compared to the corresponding manganin record. Sufficient zone density is always used to insure convergence of the results. Fifty zones per mm of PBX and the corresponding impedance matched zoning of the inert materials are used in the one-dimensional calculations reported here. Table 2 lists the equation of state and reaction rate parameters used in the Ignition and Growth models for LX-10, LX-07, PBX 9501, and EDC37. Listed in Table 3 are the Gruneisen equation of state parameters for the teflon, steel, and aluminum.

COMPARISONS OF EXPERIMENTAL AND CALCULATED RESULTS

The experimental and calculated results are compared in this section by PBX in the following order: PBX 9404; LX-04; LX-10; PBX 9501; LX-07; and EDC 37.

A. As mentioned in the Experimental section, three Howitzer gun experiments were fired using PBX 9404 by Green et al.[6] The manganin gauges and reactive flow modeling were still in development at that time, but the input shock pressures and run distances to detonation are correct. The three input shock pressures were 1.2, 1.3, and 1.4 GPa. The 1.2 GPa shock did not transition to detonation in a 100 mm long target. The run distances to detonation for the 1.3 and 1.4 GPa shocks were approximately 90 mm and 70 mm, respectively. Extrapolation of the linear higher shock pressure Pop Plot for PBX 9404 in Fig. 1 yields about 30 mm for these shock pressures. These PBX 9404 run distances are included in the low pressure run distance versus shock pressure plot for the six PBX's, because they represent the upper limits of HMX PBX shock sensitivity.

B. As mentioned in the Experimental section, all five of the LX-04 experiments and corresponding modeling were published by Vandersall et al.[7] The lower limit of shock pressure that can transition to detonation within 80 mm of LX-04 was between 1.6 and 1.8 GPa, because an aluminum flyer with a velocity of 368 m/s did not cause detonation within 80 mm and an aluminum flyer with a velocity of 389 m/s caused detonation at about 65 mm. The Ignition and Growth LX-04 model parameters produced good agreement with all five experiments. The LX-04 run distances are included in the low pressure run distance versus shock pressure plots for the six PBX's, because they represent the lower limits of shock sensitivity of the three HMX/Viton PBX's.

C. Seven 101 mm gun shots were fired using LX-10. Three experimental and calculated pressure history comparisons were published by Vandersall et al.[10] The other four are listed in Table 1. One of these shots was a high shock pressure experiment, and two other experiments yielded only run distance to detonation data. So only the gauge record comparisons from shot 4717 are included here. This was the lowest shock pressure (1.7 GPa) shot and did not transition to detonation at the deepest gauge position of 40 mm. However, the reaction rate was growing rapidly. 40 mm is close to the end of the one-dimensional region so the manganin gauge

records may have been affected by side rarefaction waves. Figure 2 contains the pressure histories measured at 0, 30, 36, and 40 mm. Figure 3 contains the corresponding calculated pressure histories using the LX-10 listed in Table 2 and also used by Vandersall et al.[10] These one-dimensional calculations correctly predict a run distance to detonation of just over 40 mm, but are growing faster than the experimental records at late times. The side rarefaction waves have most likely reached the center of the charge and reduced the experimental reaction growth rate. A two-dimensional calculation of a similar LX-04 experiment demonstrated this effect.[8] All of the LX-10 run distance to detonation data is included in the comparisons for the six PBX's. Containing 95% HMX pressed to 98% TMD and formulated with an inert Viton binder, LX-10 is slightly less shock sensitive than PBX 9404.

D. Five experiments were conducted using PBX 9501. Two were reported by Chidester et al.[9] and the other three are listed in Table 1. Figure 4 shows the manganin gauge records for shot 4729, in an input shock pressure of 2.05 GPa caused detonation at 28 mm. Figure 5 contains the calculated pressure histories using the PBX 9501 parameters listed in Table 2. Figures 6 and 7 show the experimental and calculated pressure histories, respectively, for shot 4730, in which a 1.85 GPa shock caused detonation at 33.5 mm. Figures 8 and 9 contain the experimental and calculated pressure histories, respectively, for Howitzer shot HG08-01, in which a 1.6 GPa pressure caused a transition to detonation at 53 mm. A previously reported Howitzer shot HG07-02 with a shock pressure of 1.45 GPa transitioned to detonation at 72 mm.[9] Good agreement was obtained between the experimental and calculated pressure histories in all five PBX 9501 experiments. PBX 9501 exhibits a lower than shock sensitivity than PBX 9404 and LX-10, the other two PBX's with 94 – 95% HMX. This is due to its plasticizer/binder, which is less reactive than PBX 9404's nitrocellulose containing binder and more pliable than the Viton binder in LX-10. Softer, more pliable binders are known to flow better during shock compression. This results in less work done and less localized heating, creating fewer reacting hot spots.[22]

E. LX-07 with 90% HMX and 10% Viton is expected to be intermediate in shock sensitivity between LX-04 (85% HMX/15% Viton) and LX-10 (95% HMX/5% Viton). Six LX-07 experiments were

fired and are listed in Table 1. Shots 4735 and 4736 are higher shock pressure experiments whose run distances to detonation agree with previous Pop Plot data on LX-07. The other four experiments extend the LX-07 run distance data to lower shock pressures. Figures 10 and 11 show the experimental and calculated pressure histories (using the LX-07 Ignition and Growth parameters listed in Table 2), respectively, for shot 4737, in which a 2.25 GPa shock pressure results in a 23.5 mm run distance to detonation. Figures 12 and 13 compare the experimental and calculated pressure histories, respectively, for shot 4738, in which a 1.8 GPa shock transitions to detonation at 34 mm. Figures 14 and 15 contain the experimental and calculated pressure histories, respectively, for Howitzer shot HG08-03, in which a 1.65 GPa shock transitioned to detonation at 61 mm. Figures 16 and 17 show the experimental and calculated pressure histories, respectively, for Howitzer shot HG07-01, in which a 1.55 GPa shock did not detonate in the 80 mm long LX-07 target. Good agreement between experiment and modeling was obtained for all four experiments. LX-07 is intermediate in shock sensitivity between LX-04 and LX-10 at low shock pressures.

F. EDC37 with 91% HMX was expected to be similar to LX-07 in low pressure shock sensitivity, but its oily binder allows it to be pressed to near TMD. Thus only a small void volume (0.2%) is available to form reactive hot spots.[23] Four Howitzer gun shots fired using EDC 37 are listed in Table 1, and three of them at approximately 1.7, 1.9 and 2.1 GPa did not detonate within the 80 mm run distance. The fourth shot with a shock pressure of approximately 2.4 GPa resulted in a transition to detonation at 69 mm. The Ignition and Growth model parameters for EDC37 in Table 2 are based on the other HMX based PBX's and higher pressure embedded particle velocity gauge experiments.[23] Figures 18 and 19 contain the experimental and calculated pressure histories, respectively, for shot HG07-03, which had a shock pressure of 1.7 GPa. The manganin gauges show some pressure increases, although, at late times, there is most likely two-dimensional gauge stretching, while the calculations show no growth. Figures 20 and 21 show the experimental and calculated pressure histories, respectively, for shot HG07-04, which has an initial pressure of 1.9 GPa. The gauge records and calculations show reaction growth to pressures of about 10 GPa. Figures 22 and 23 contain the experimental and calculated

pressure histories, respectively, for shot HG07-05, which had a shock pressure of 2.1 GPa. In both the experiment and calculations, the pressures are rapidly growing but the transition to detonation does not occur within the 80 mm long charge. Figures 24 and 25 show the experimental and calculated pressure histories, respectively, for shot HG08-02, which has an initial pressure of 2.4 GPa. The experimental records show a transition to detonation just before the 70 mm gauge position, while the calculations show a transition just after the 70 mm deep gauge. These agreements between the calculated and experimental pressure histories were obtained by using: a larger critical compression required for hot spot ignition of EDC37 relative to the other HMX PBX's; a smaller value of Figmax = 0.002 corresponding to the lower void fraction in EDC 37;[23] and a slower growth coefficient G_1 for fewer spreading hot spots,

The lower shock pressure experiments on the six HMX based PBX's clearly show much longer run distances to detonation as the critical pressure for detonation transition is approached than predicted by extrapolation of high pressure Pop Plots. Figure 26 shows all of the run distances to detonation caused by shock pressures below 3 GPa measured for the six HMX PBX's in this and the previous studies.[6,7,9,10] The effects of initial void volume, HMX percentage, and type of binder are more pronounced than they are at higher shock pressures.

CONCLUSIONS

Measured run distances to detonation at relatively low input shock pressures for six HMX based PBX's are considerably longer than those predicted by extrapolations of linear Pop Plot fits to higher shock pressure data. Embedded manganin pressure gauges measured the growth of hot spot reactions in these experiments. These pressure histories, together with the run distance to detonation data, are used to extend existing Ignition and Growth reactive flow models to these lower shock pressures. The main changes in the model parameters are the use of non-zero values of the critical compression compressions required for hot spot ignition. These critical compressions range from approximately 0.07 to 0.09, corresponding to shock pressures of about 1 GPa to 1.4 GPa. These minimum shock pressures for SDT are close to those estimated by previous shock initiation studies on HMX based PBX's.[6,7,24-26.]

The effects of HMX percentage, porosity, and binder compressibility are shown to be the same as in higher shock pressure initiation of HMX PBX's but perhaps even more important. For EDC37, which

has an order of magnitude less porosity than the other five HMX based PBX's, the low shock pressure sensitivity is greatly reduced. At approximately the same initial porosity, the higher the HMX percentage, the greater is the shock sensitivity. With approximately the same porosity and HMX percentage, the HMX based PBX's with more compressible binder/plasitcizer components, such as PBX 9501 and EDC37, are less shock sensitive than those with the stiffer Viton binder. These trade-offs in PBX formulation strength, performance, and sensitvity must always be taken into account when formulating large explosive charges.

Some of the main products of this research are the low shock pressure Ignition and Growth reactive flow model parameters for HMX based PBX's that can be used to predicted shock initiation or failure of initiation in large explosive charges that cannot be tested experimentally due to cost, explosive weight limits, or other limitations. There are many scenarios in which large, relatively slow moving fragments can impact bare or covered, confined or unconfined HMX based PBX charges producing low pressure shock waves that may cause SDT after several centimeters of propagation. The Ignition and Growth model parameters normalized to these one-dimensional experiments are conservative, because any two-dimensional pressure relief effects will decrease the shock pressure and the shock duration time, making the explosive charge less likely to react. While hazard and vulnerability scenarios that are predicted to be close to shock initiation thresholds should always be experimentally verified if possible, the application of well normalized reactive flow models can be greatly reduce the number of costly experiments in evaluating potential low shock pressure threats to large explosive charges.

ACKNOWLEDGMENTS

The 101 mm and 155 mm gun crews are thanked for their excellent work building and firing these experiments. This work was performed under the auspices of the United States Department of Energy by the Lawrence Livermore National Laboratory under Contract No. DE-AC52-07NA2734.

TABLE 1. NEW EXPERIMENTS FIRED USING LX-10, PBX 9501, LX-07, AND EDC 37

SHOT NUMBER	IMPACT VELOCITY(km/s)	FLYER PLATE	IMPACT PLATE	PRESSURE (GPa)	RUN TO DET (mm)
A. LX-10					
4717	625	Teflon	Teflon	1.7	>40
4725	950	Aluminum	Aluminum	4.8	6.7
4726	943	Teflon	Teflon	2.9	20.5
4727	733	Teflon	Teflon	2.1	30.8
B. PBX 9501					
4729	711	Teflon	Teflon	2.05	28
4730	654	Teflon	Teflon	1.85	33.5
HG08-01	378	Aluminum	Aluminum	1.6	52.8
C. LX-07					
4735	973	Aluminum	Aluminum	5.0	4.0
4736	1006	Teflon	Teflon	3.1	12
4737	784	Teflon	Teflon	2.25	23.5

4738	664	Teflon	Teflon	1.8	34
HG07-01	349	Aluminum	Aluminum	1.55	>80
HG08-03	385	Aluminum	Aluminum	1.65	61
D. EDC 37					
HG07-03	391	Aluminum	Aluminum	1.7	>80
HG07-04	429	Aluminum	Aluminum	1.9	>80
HG07-05	483	Aluminum	Aluminum	2.1	>80
HG08-02	519	Aluminum	Aluminum	2.4	69

TABLE 2. IGNITION AND GROWTH PARAMETERS FOR LX-10, LX-07, PBX 9501, AND EDC37

A. LX-10 ρ_o =1.862 g/cm^3

UNREACTED JWL	PRODUCT JWL	REACTION RATES
A=952200 GPa	A=880.7 GPa	I=20000 μs^{-1}
B= -5.944 GPa	B=18.36 GPa	a=0.0794
R_1=14.1	R_1=4.62	b=0.667
R_2=1.41	R_2=1.32	x=4.0 F_{igmax}=0.02
ω=0.8867	ω=0.38	G_1=0.025 GPa$^{-2}\mu s^{-1}$
C_V=2.7806x10^{-3} GPa/K	C_V=1.0x10^{-3} GPa/K	c=0.667
T_o = 298$^\bullet$K	E_o=10.4GPa	d=0.667
Shear Modulus=5.0 GPa		y=2.0 F_{G1max}=0.5
Yield Strength=0.2 GPa		G_2=0.00032 GPa$^{-3}\mu s^{-1}$
		e=0.333 z=3.0
		g=1.0 FG2min=0.5

B. PBX 9501 ρ_o =1.832 g/cm^3

UNREACTED JWL	PRODUCT JWL	REACTION RATES
A=732000 GPa	A=1668.9GPa	I=20000 μs^{-1}
B= -5.2654 GPa	B=59.69GPa	a=0.0819
R_1=14.1	R_1=5.9	b=0.667
R_2=1.41	R_2=2.1	x=4.0 F_{igmax}=0.02
ω=0.8867	ω=0.45	G_1=0.027 GPa$^{-2}\mu s^{-1}$
C_V=2.7806x10^{-3} GPa/K	C_V=1.0x10^{-5} GPa/K	c=0.667
T_o = 298$^\bullet$K	E_o=10.2 GPa	d=0.667
Shear Modulus=3.54 GPa		y=2.0 F_{G1max}=0.5
Yield Strength=0.2 GPa		G_2=0.00032 GPa$^{-1}\mu s^{-1}$
		e=0.333 z=3.0
		g=1.0 F_{G2min}=0.5

C. LX-07 ρ_o =1.850 g/cm^3

UNREACTED JWL	PRODUCT JWL	REACTION RATES
A=952200 GPa	A=871.0GPa	$I=20000\ \mu s^{-1}$
B= -5.944 GPa	B=13.9 GPa	a=0.07117
R_1=14.1	R_1=4.6	b=0.667
R_2=1.41	R_2=1.15	x=4.0 F_{igmax}=0.02
ω=0.8867	ω=0.3	$G_1=0.0285\ GPa^{-3}\mu s^{-1}$
$C_V=2.7806x10^{-3}$ GPa/K	$C_V=1.0x10^{-3}$ GPa/K	c=0.667
T_o = 298°K	E_o=10.4 GPa	d=0.667
Shear Modulus=5.0 GPa		y=2.0 F_{G1max}=0.5
Yield Strength=0.2 GPa		$G_2=0.00032\ GPa^{-1}\mu s^{-1}$
		e=0.333 z=3.0
		g=1.0 FG2min=0.5

D. EDC37 $\rho_o = 1.841\ g/cm^3$

UNREACTED JWL	PRODUCT JWL	REACTION RATES
A=732000 GPa	A=1668.9 GPa	$I=20000\ \mu s^{-1}$
B= -5.2654 GPa	B=59.69 GPa	a=0.09114
R_1=14.1	R_1=5.9	b=0.667
R_2=1.41	R_2=2.1	x=4.0 F_{igmax}=0.002
ω=0.8867	ω=0.45	$G_1=0.012\ GPa^{-2}\mu s^{-1}$
$C_V=2.7806x10^{-3}$ GPa/K	$C_V=1.0x10^{-3}$ GPa/K	c=0.667
T_o = 298°K	E_o=10.2 GPa	d=0.667
Shear Modulus=3.54 GPa		y=2.0 F_{G1max}=0.5
Yield Strength=0.2 GPa		$G_2=0.00032\ GPa^{-3}\mu s^{-1}$
		e=0.333 z=3.0
		g=1.0 F_{G2min}=0.5

TABLE 3. GRUNEISEN EQUATION OF STATE PARAMETERS FOR ALUMINUM, STEEL, AND TEFLON

$$P = \rho_o c^2 \mu[1+(1-\gamma_o/2)\mu - a/2\mu^2]/[1-(S_1-1)\mu - S_2\mu^2/(\mu+1) - S_3\mu^3/(\mu+1)^2]^2 + (\gamma_o + a\mu)E,$$

where $\mu = (\rho/\rho_o - 1)$ and E is thermal energy

INERT	ρ_o(g/cm^3)	c(mm/μs)	S_1	S_2	S_3	γ_o	a
Al 6061	2.703	5.24	1.4	0.0	0.0	1.97	0.48
Steel	7.90	4.57	1.49	0.0	0.0	1.93	0.5
Teflon	2.15	1.68	1.123	3.983	-5.797	0.59	0.0

REFERENCES

1. J. B. Ramsey and A. Popolato, Fourth Symposium (International) on Detonation, Office of Naval Research ACR-126, White Oak, MD, 1965, p. 233.

2. A. M. Weston, J. F. Kincaid, E. James, E. L. Lee, L. G. Green, and J. R. Walton, Seventh Symposium (International) on Detonation, Naval Surface Warfare Center NSWC MP82-334, Annapolis, MD, 1981, p. 887.

3. J. W. Forbes, C. M. Tarver, P. A. Urtiew, and F. Garcia, Eleventh International Detonation Symposium, Office of Naval Research ONR 33300-5, Snowmass, CO, 1999, p. 145.

4. S. A. Sheffield, R. L. Gustavsen, L. G. Hill, and R. Alcon, Eleventh International Detonation Symposium, Office of Naval Research ONR 33300-5, Snowmass, CO, 1999, p. 451.

5. C. M. Tarver, J. W. Forbes, F. Garcia, and P. A. Urtiew, Shock Compression of Condensed Matter-2001, AIP Conference 620, Atlanta, GA, 2002, p. 1043.

6. L. Green, E. Nidick, E. Lee, and C. Tarver, Symposium on High Dynamic Pressures, French Atomic Energy Commission, Paris, France, 1978, p.115.

7. C. M. Tarver, J. O. Hallquist, and L. M. Erickson, Eighth Symposium (International) on Detonation, Naval Surface Weapons Center NSWC MP86-194, Albuquerque, NM, 1985, p. 951.

8. K. S. Vandersall, C. M. Tarver, F. Garcia,, S. K. Chidester, P. A. Urtiew, and J. W. Forbes, Thirteenth International Detonation Symposium, Office of Naval Research ONR 351-07-2, Norfolk, VA, 2006, p. 904.

9. S. K. Chidester, D. G. Thompson, K. S. Vandersall, D. J. Idar, C. M. Tarver, F. Garcia, and P. A. Urtiew, Shock Compression of Condensed Matter – 2007, AIP Conference Proc. 955, Waikoloa, Hawaii, 2007, p. 903.

10. K. S. Vandersall, C. M. Tarver, F. Garcia, P. A. Urtiew, and S. K. Chidester, Shock Compression of Condensed Matter – 2007, AIP Conference Proc. 955, Waikoloa, Hawaii, 2007, p. 1010.

11. G. de Oliveira, A.K. Kapila, W, Schwendeman, J. B. Bdzil, W. D. Henshaw, and C. M. Tarver, Thirteenth International Detonation Symposium, Office of Naval Research ONR 351-07-2, Norfolk, VA, 2006, p. 13.

12. M. L. Garcia and C. M. Tarver, Thirteenth International Detonation Symposium, Office of Naval Research ONR 351-07-2, Norfolk, VA, 2006, p. 63.

13. P. A. Urtiew, K. S. Vandersall, C. M. Tarver, F. Garcia, and J. W. Forbes, Thirteenth International Detonation Symposium, Office of Naval Research ONR 351-07-2, Norfolk, VA, 2006, p. 929.

14. C. M. Tarver, Propellants, Explosives, Pyrotechnics **30,** 109 (2005).

15. C. M. Tarver and E. M. McGuire, Twelfth International Detonation Symposium, Office of Naval Research ONR-333-05-2, San Diego, CA, 2002, p. 641.

16. B. Hayes and C. M. Tarver, Seventh Symposium (International) on Detonation, Naval Surface Warfare Center NSWC MP82-334, Annapolis, MD, 1981, p. 1029.

17. C. M. Tarver, J. W. Kury, and R. D. Breithaupt, J. Applied Physics **82**, 3771 (1997).

18. C. M. Tarver, W. C. Tao, and C. G. Lee, Propellants, Explosives, Pyrotechnics, **21**, 238 (1996).

19. L. G. Green, C. M. Tarver, and D. L. Erskine, Ninth Symposium (International) on Detonation, Office of the Chief of Naval Research, OCNR 113291-7, Portland, OR, 1989, p. 670.

20. A. L. Nichols III and C. M. Tarver, Twelfth International Detonation Symposium, Office of Naval Research ONR-333-05-2, San Diego, Ca, 2002, p. 489.

21. S. K. Chidester, K. S. Vandersall, L. L. Switzer, and C. M. Tarver, Shock Compression of Condensed Matter – 2005, AIP Conference Proc. 845, Baltimore, MD, 2005, p. 1049.

22. S. Lecume, P. Gimenez, J. Mala, and J. F. Guery, Tenth International Detonation Symposium, Office of Naval Research ONR 33395-12, Boston, MA, 1993, p. 898.

23. R. L. Gustavsen, S. A. Sheffield, R. R. Alcon, L. G. Hill, R. E. Winter, D. A. Salisbury, and P. Taylor, Shock Compression of Condensed Matter-1999, AIP Conference Proc. 505, Snowbird, UT, 2000, p. 879.

24. J. Wackerle, R. L. Rabie, M. J. Ginsberg, and A. B. Anderson, Symposium on High Dynamic Pressures, French Atomic Energy Commission, Paris, France, 1978, p.127.

25. J. J. Dick, A. R. Martinez, and R. S. Hixon, Eleventh International Detonation Symposium, Office of Naval Research ONR 33300-5, Snowmass, CO, 1999, p. 317.

26. C. M. Tarver, P. A. Urtiew, S. K. Chidester, and L. G. Green, Propellants, Explosives, Pyrotechnics 18, 117 (1993).

FIGURE CAPTIONS

Figure 1. High shock pressure Pop Plots for several HMX PBX's

Figure 2. Experimental pressure histories for LX-10 shocked to 1.7 GPa

Figure 3. Calculated pressure histories for LX-10 shocked to 1.7 GPa

Figure 4. Experimental pressure histories for PBX 9501 shocked to 2.05 GPa

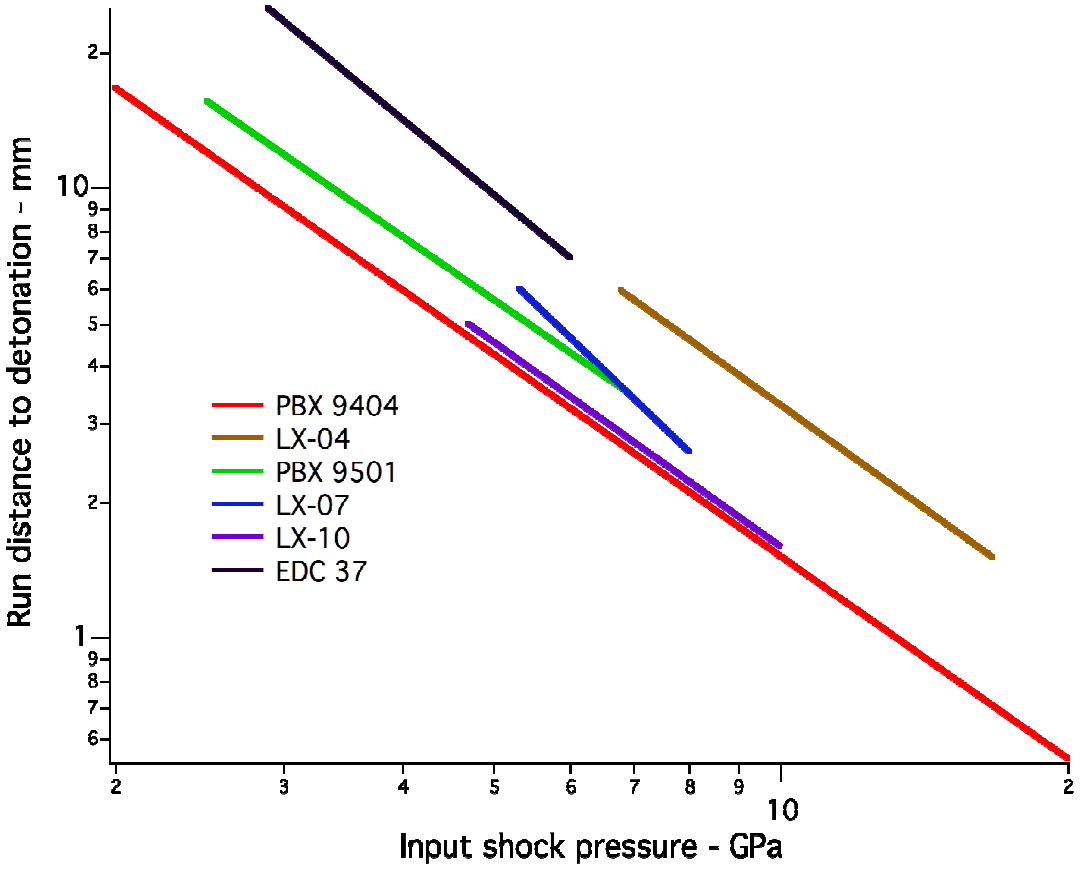

Figure 1. High shock pressure Pop Plots for several HMX PBX's

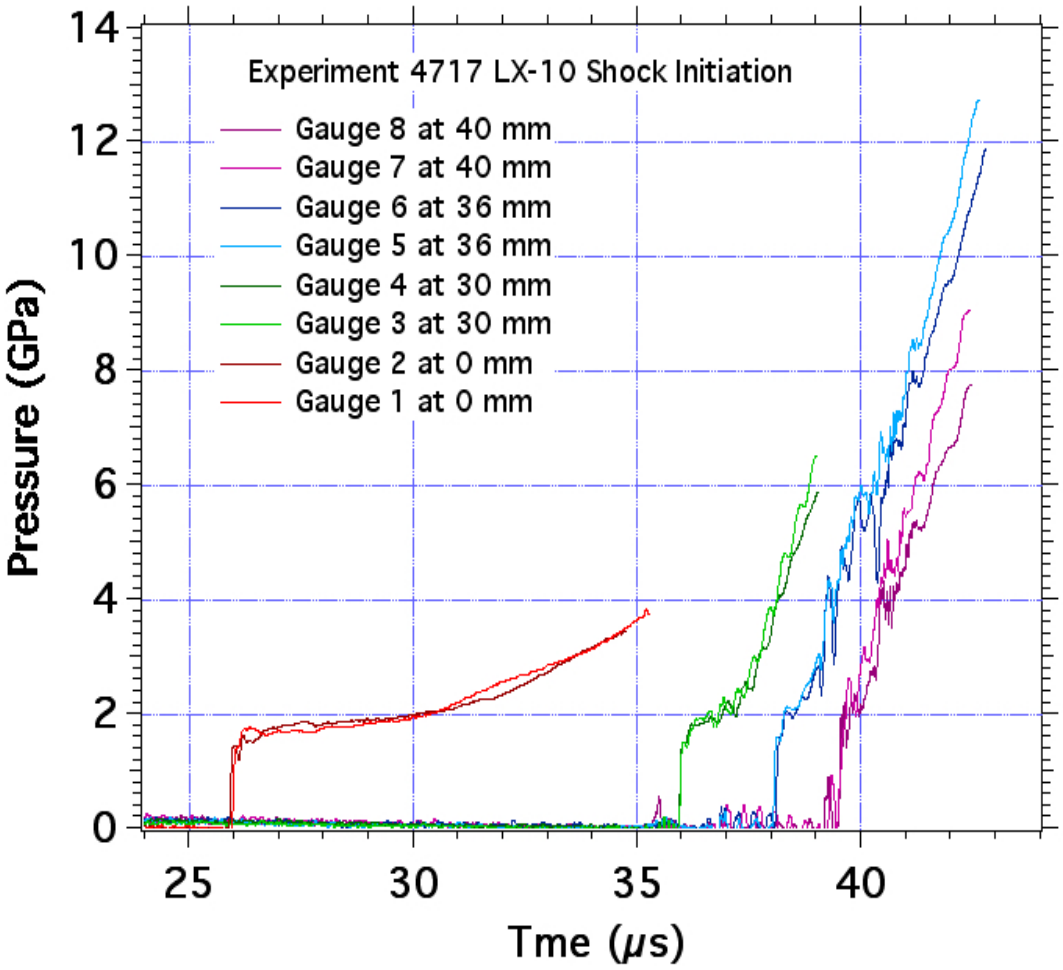

Figure 2. Experimental pressure histories for LX-10 impacted at 1.7 GPa

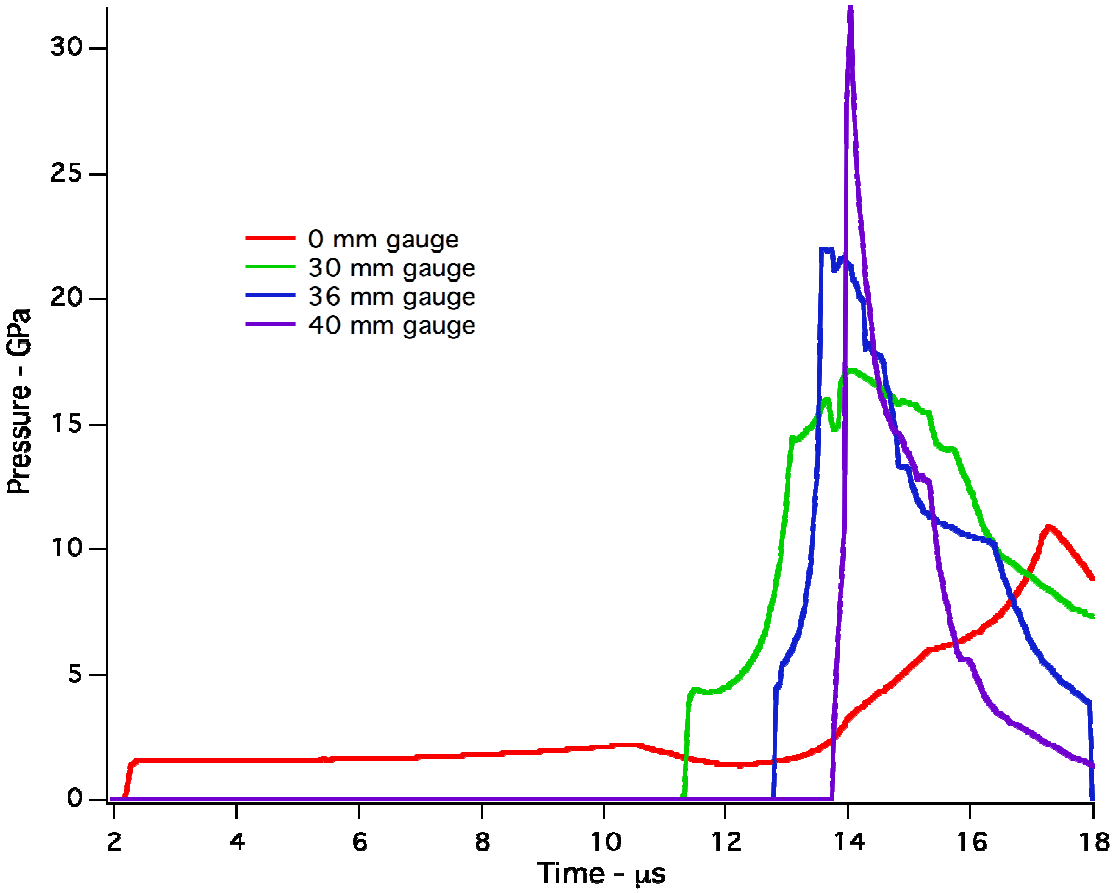

Figure 3. Calculated pressure histories for LX-10 impacted at 1.7 GPa

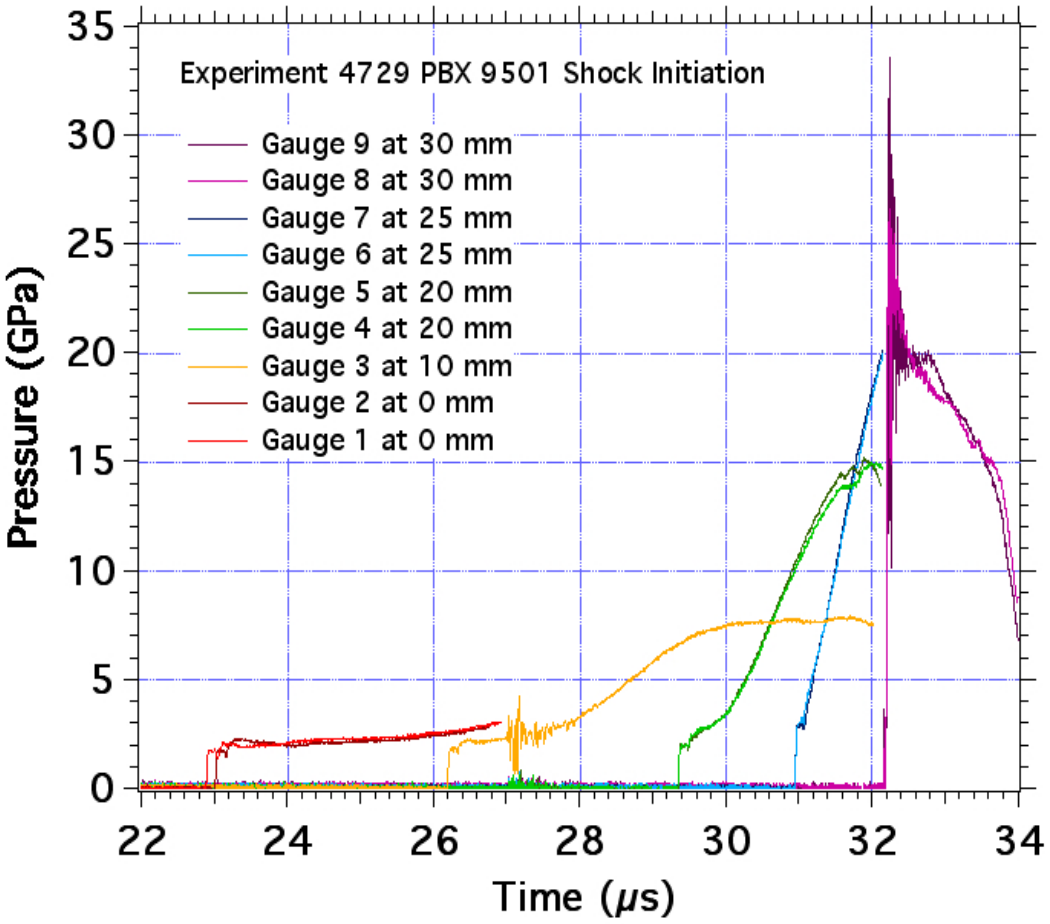

Figure 4. Experimental pressure histories for PBX 9501 impacted at 2.05 GPa

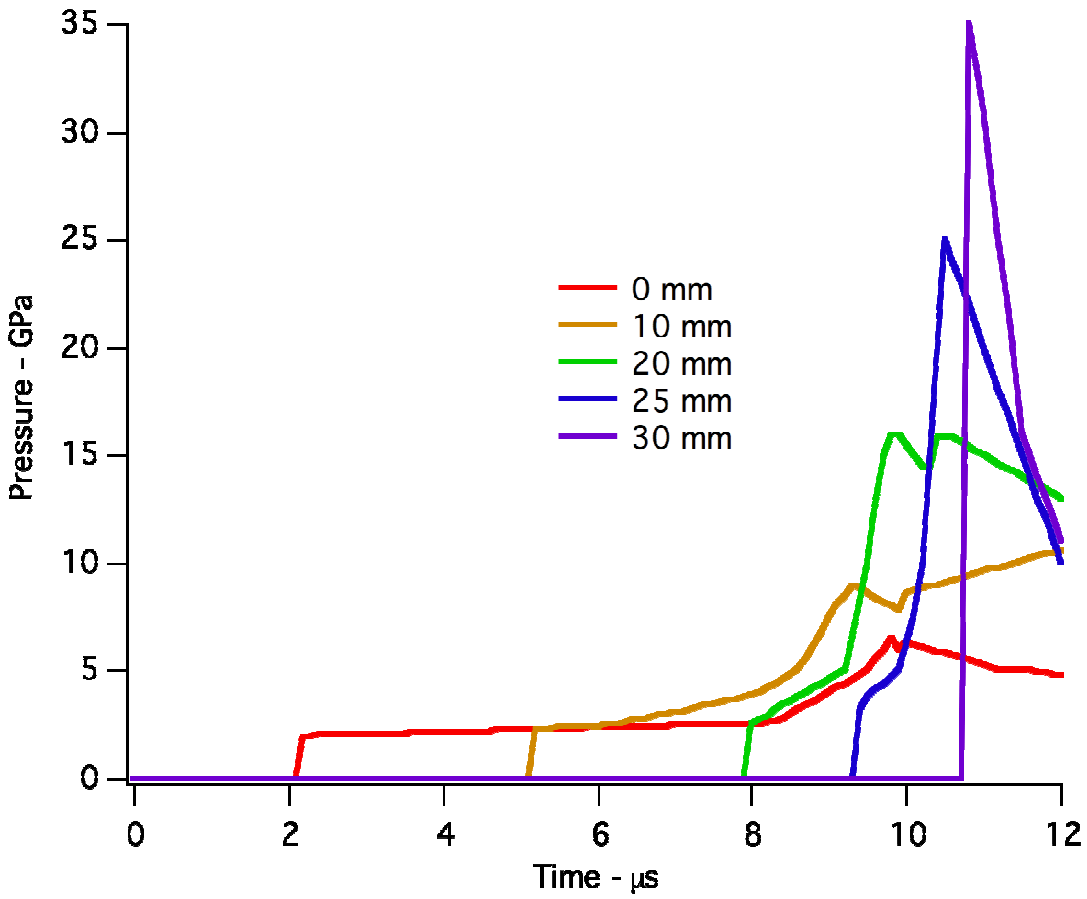

Figure 5. Calculated pressure histories for PBX 9501shock to 2.05 GPa

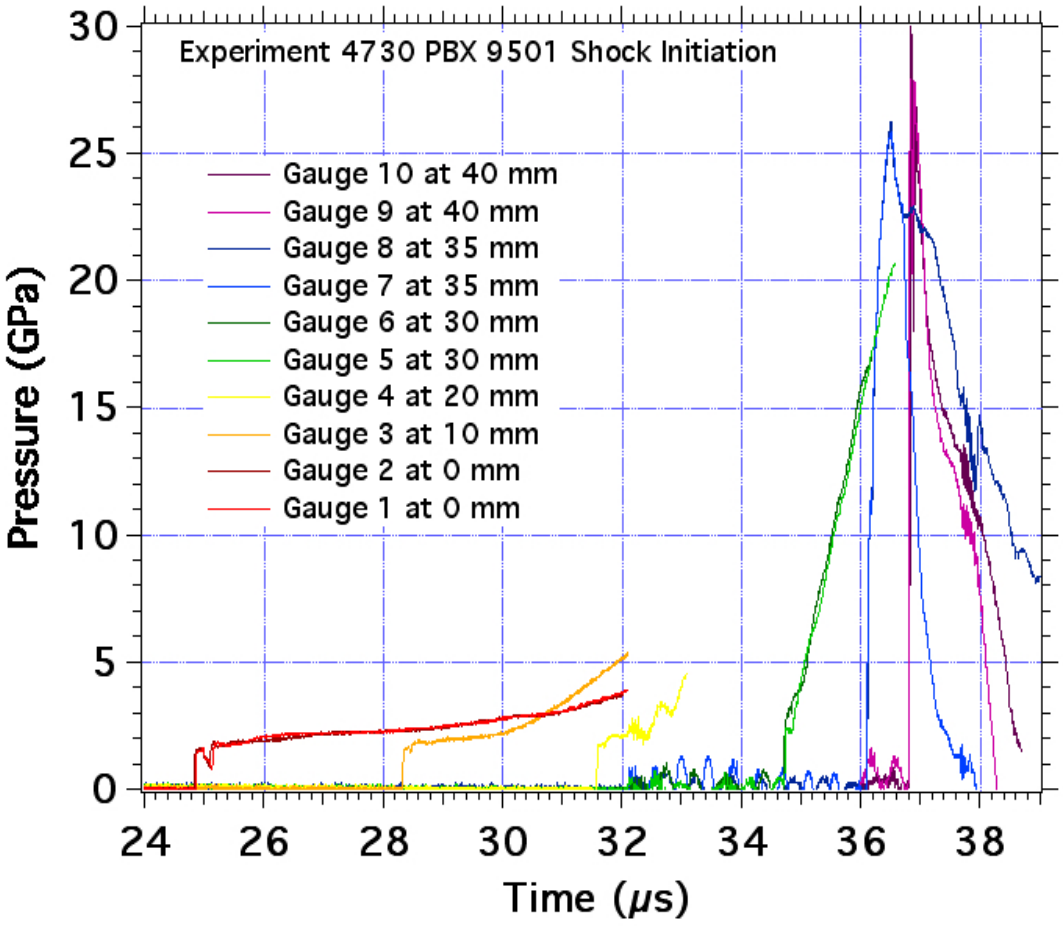

Figure 6. Experimental pressure histories for PBX 9501 impacted at 1.85 GPa

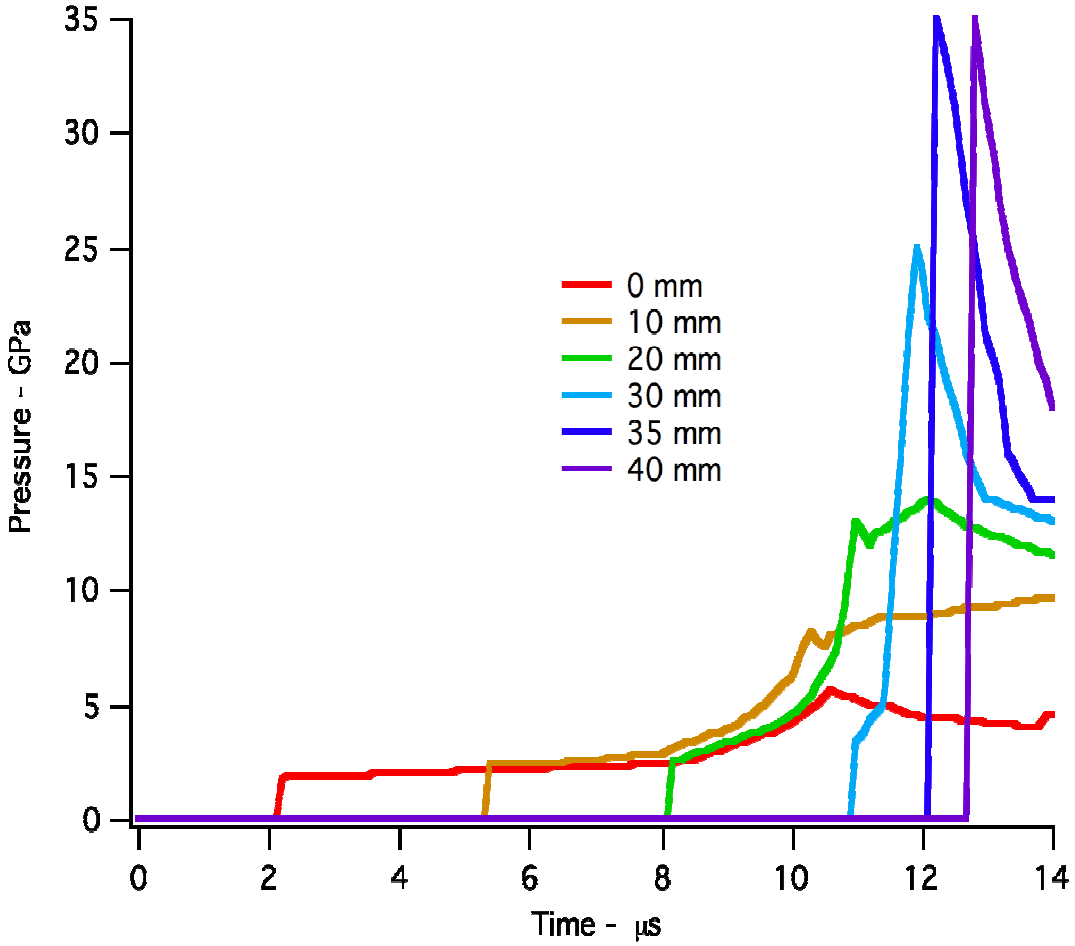

Figure 7. Calculated pressure histories for PBX 9501 shocked to 1.85 GPa

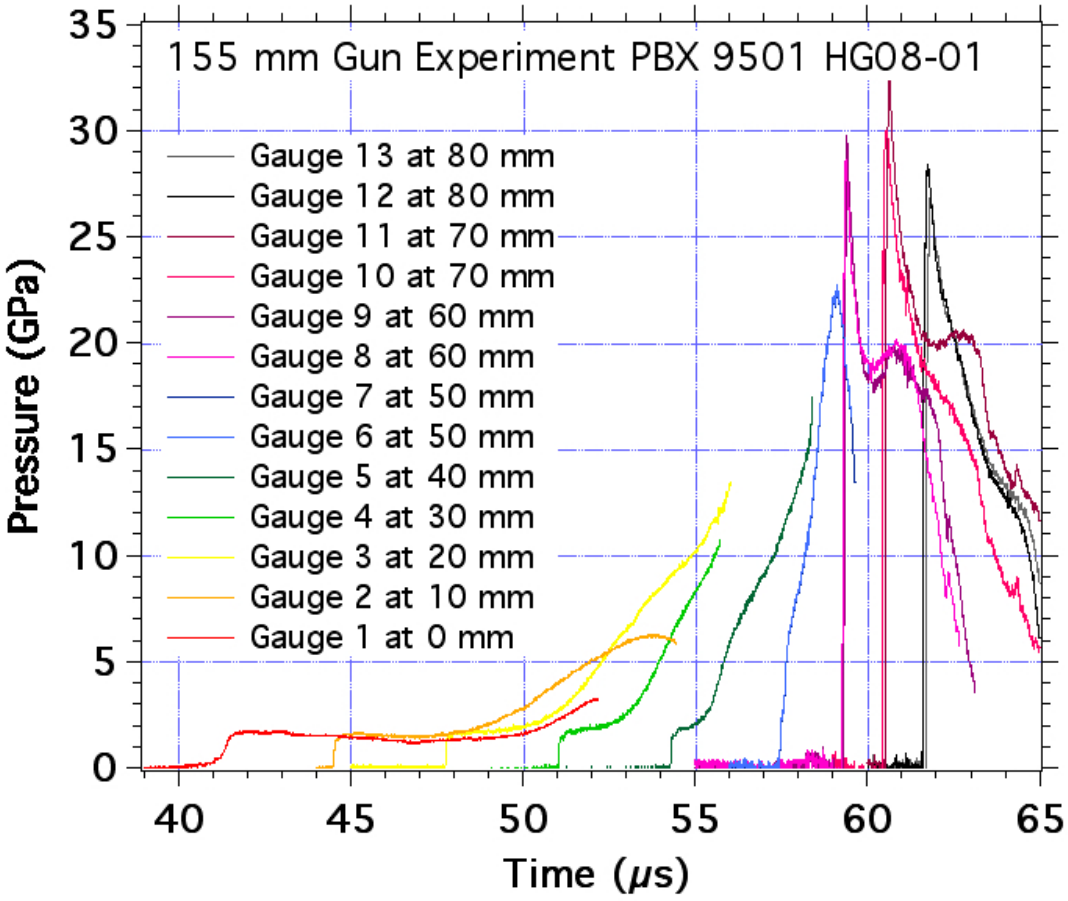

Figure 8. Experimental pressure histories for PBX 9501 shocked to 1.6 GPa

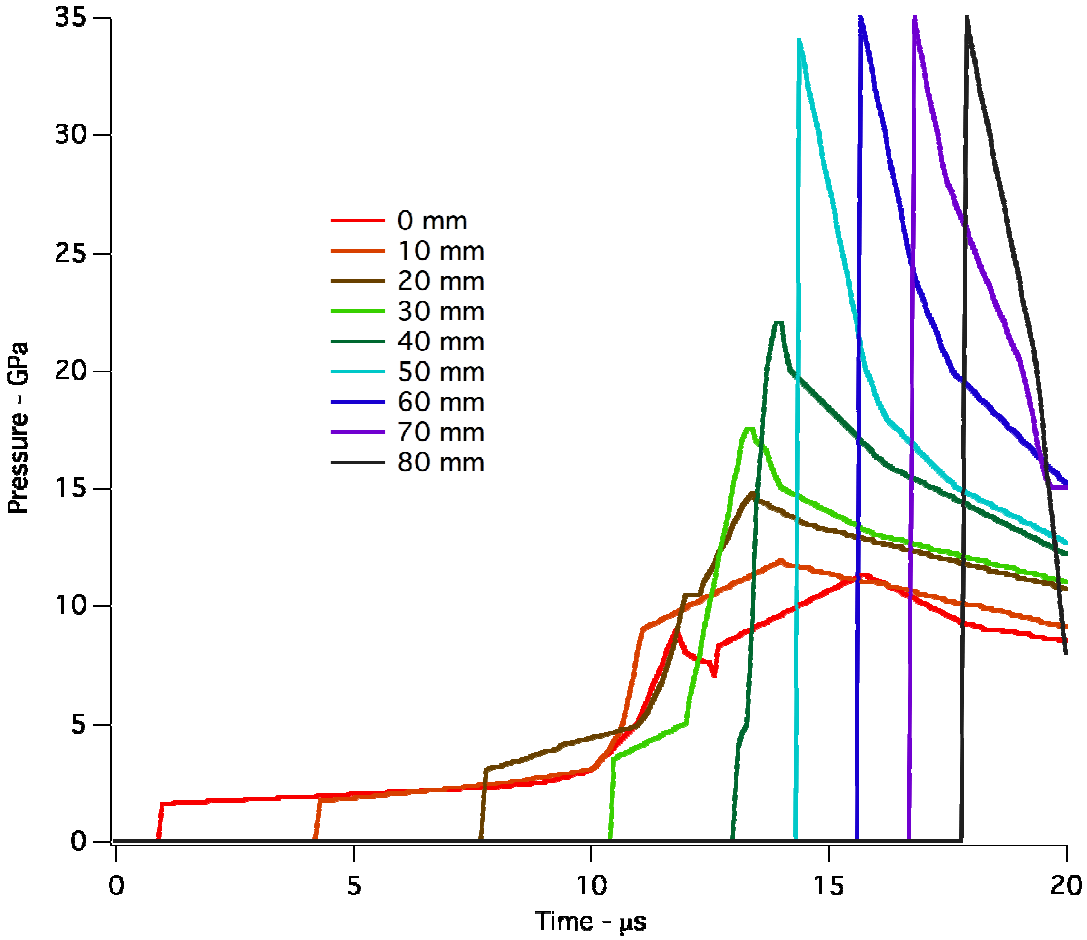

Figure 9. Calculated pressure histories for PBX 9501 shocked to 1.6 GPa

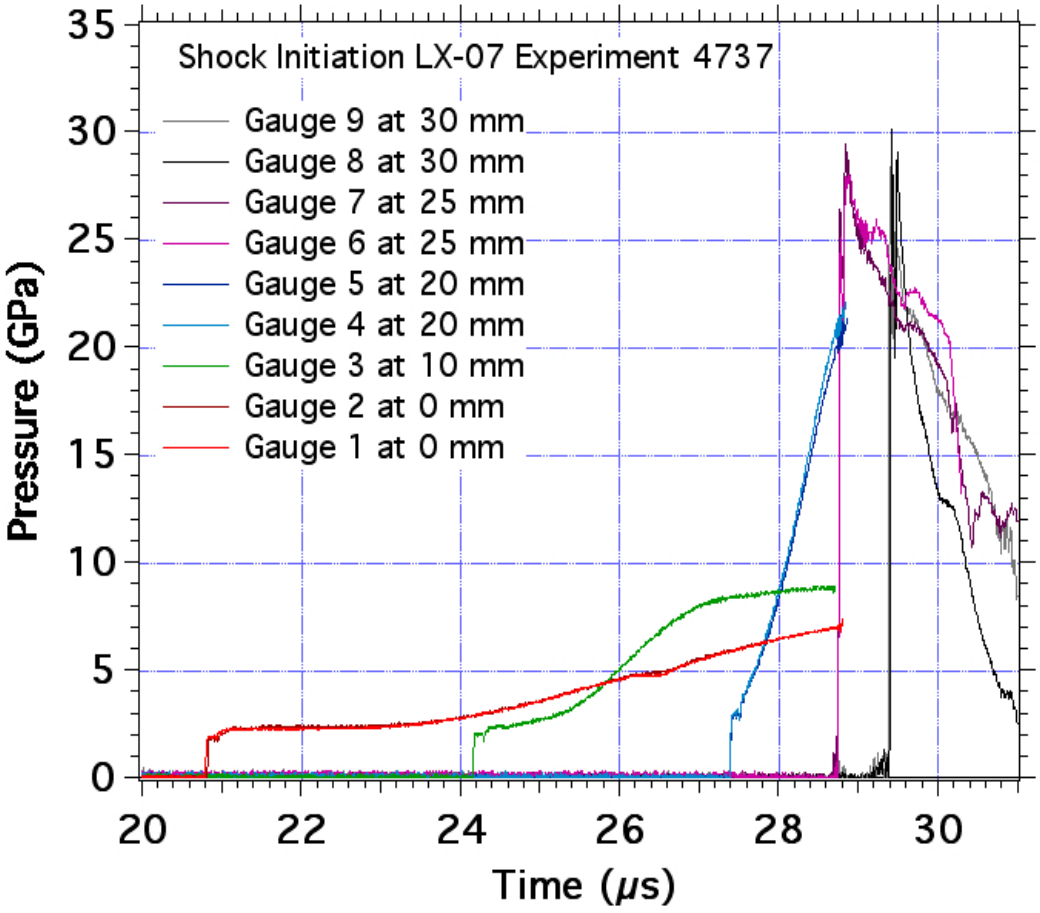

Figure 10. Experimental pressure histories for LX-07 shocked to 2.25 GPa

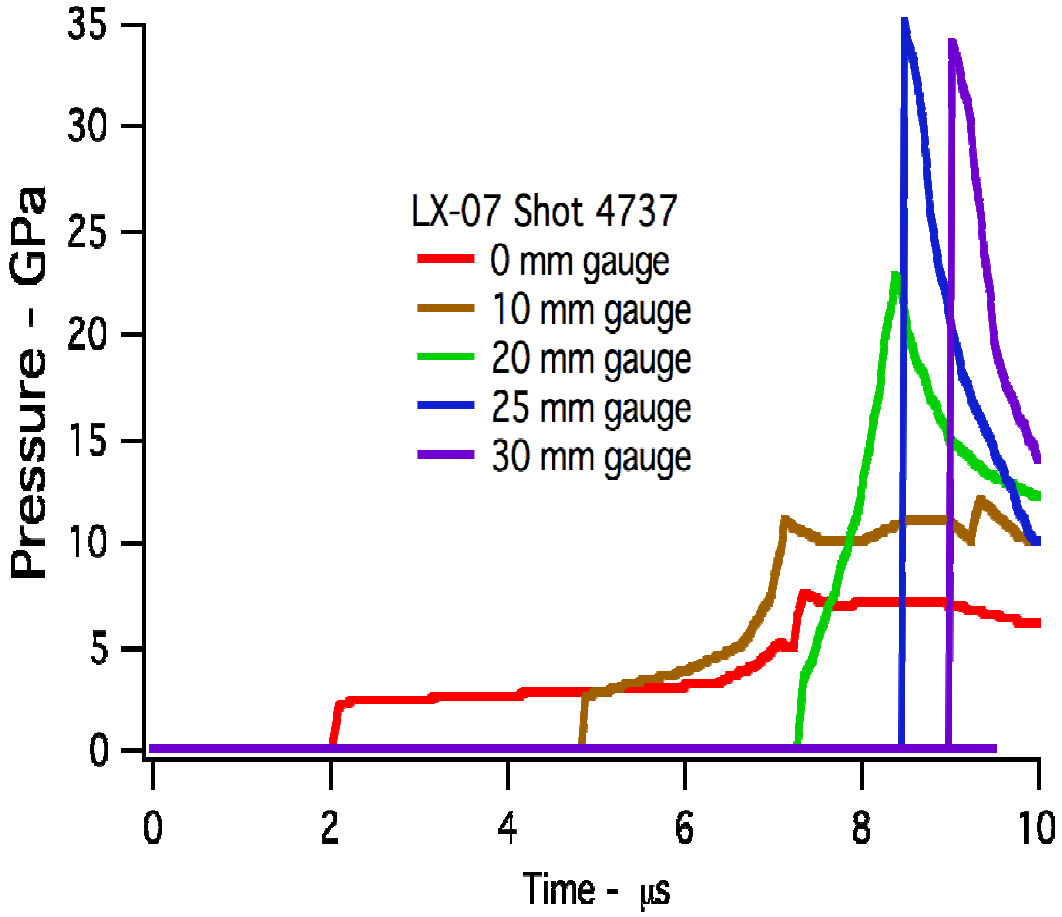

Figure 11. Calculated pressure histories for LX-07 shocked to 2.25 GPa

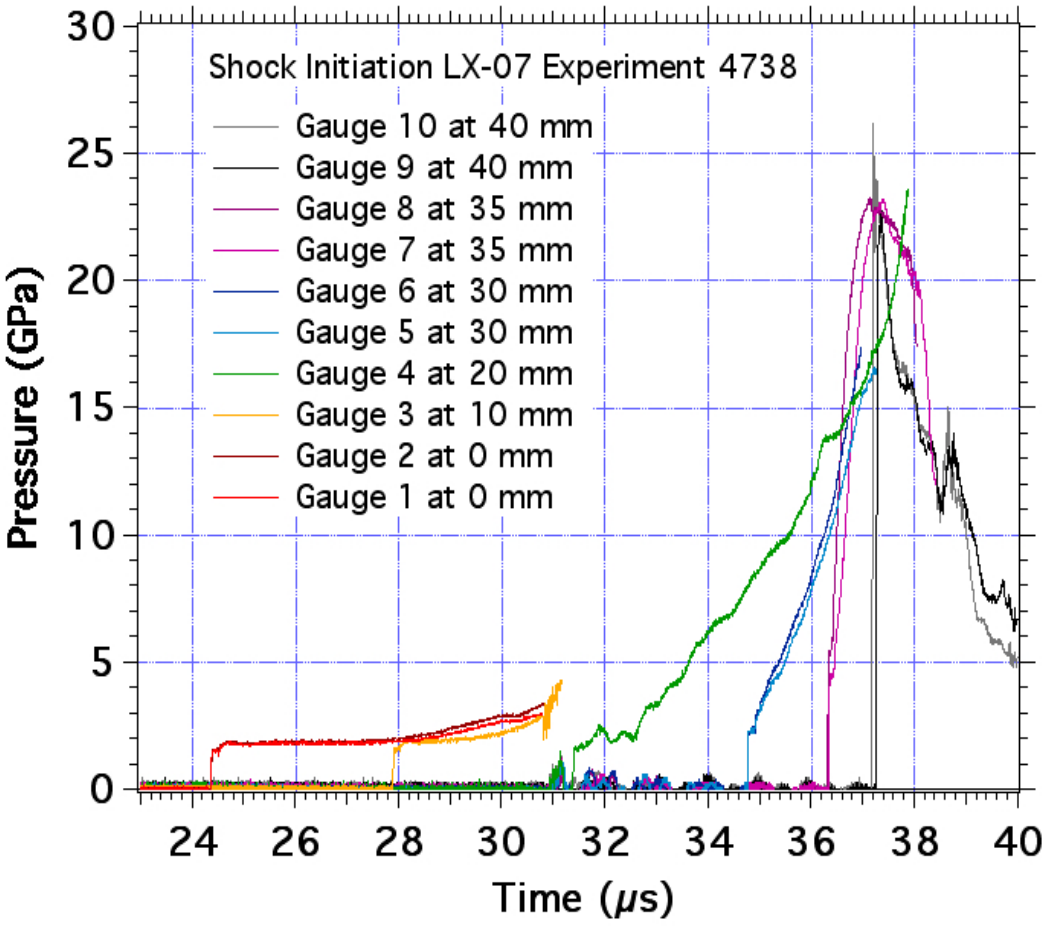

Figure 12. Experimental pressure histories for LX-07 shocked to 1.8 GPa

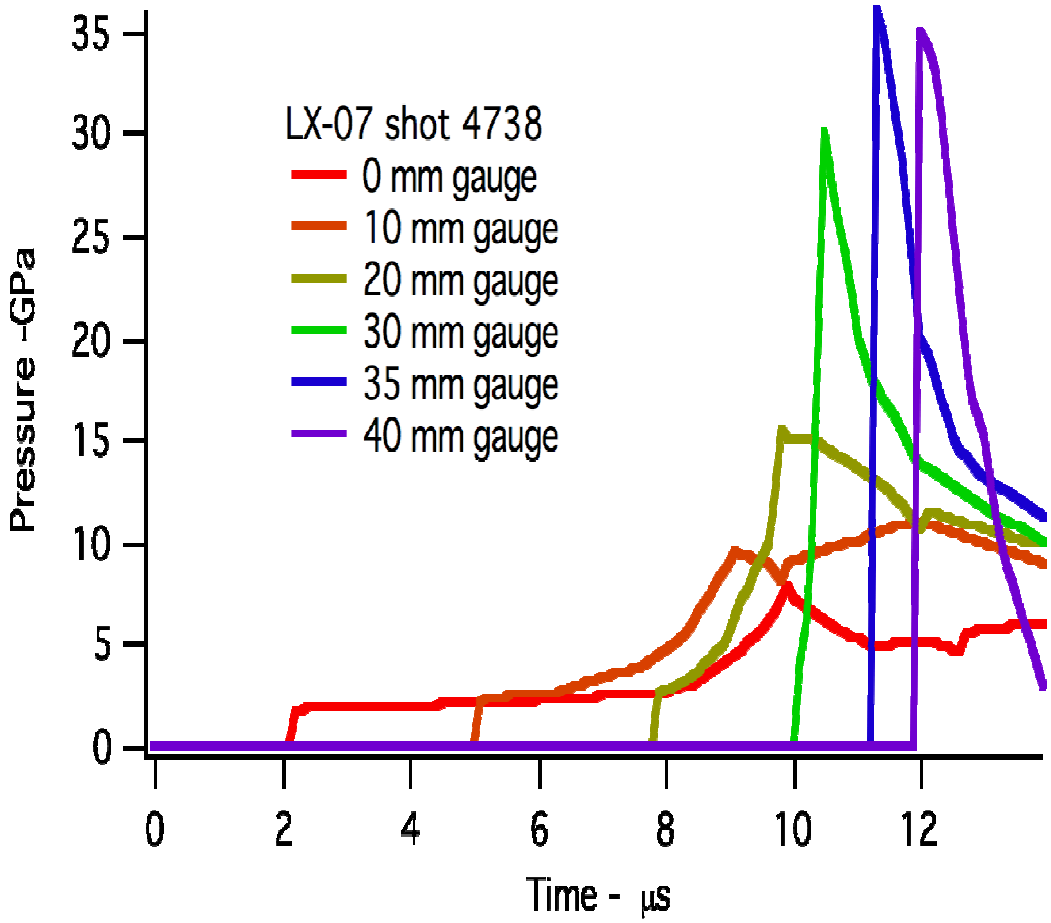

Figure 13. Calculated pressure histories for LX-07 shocked to 1.8 GPa

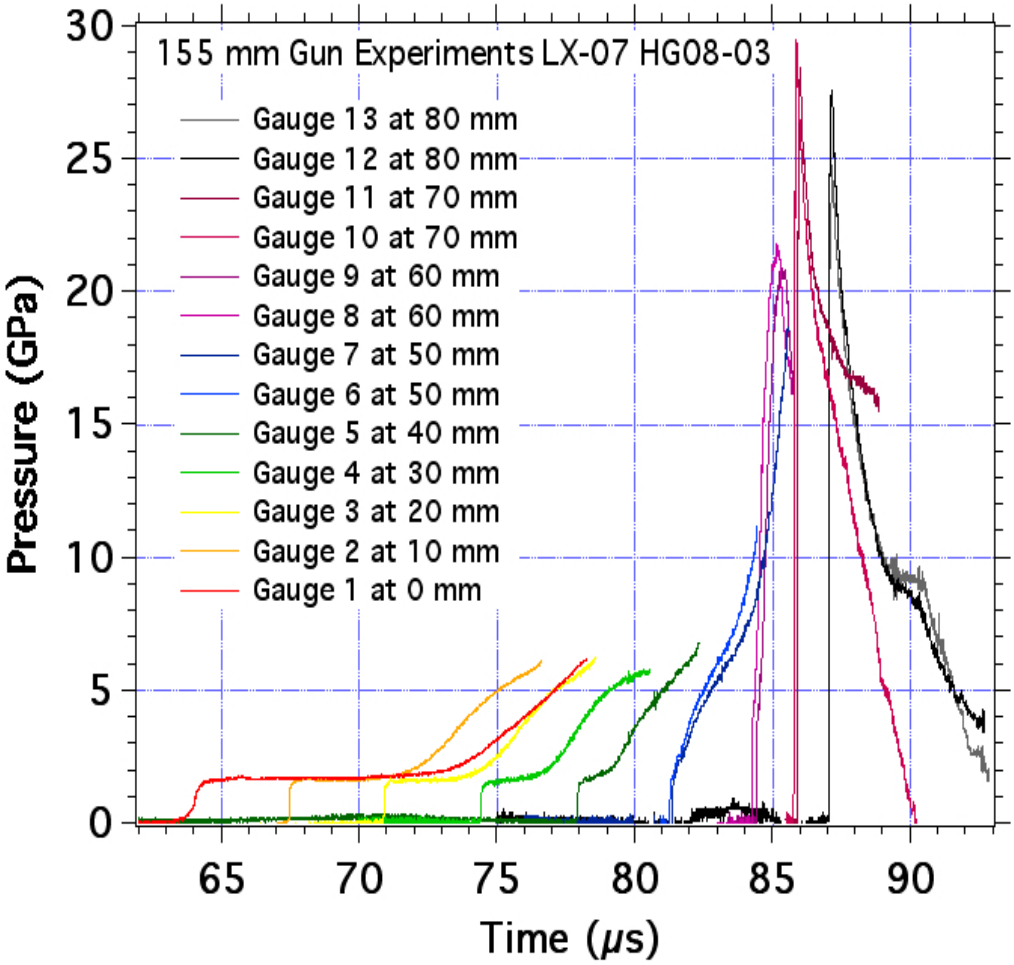

Figure 14. Experimental pressure histories for LX-07 shocked to 1.65 GPa

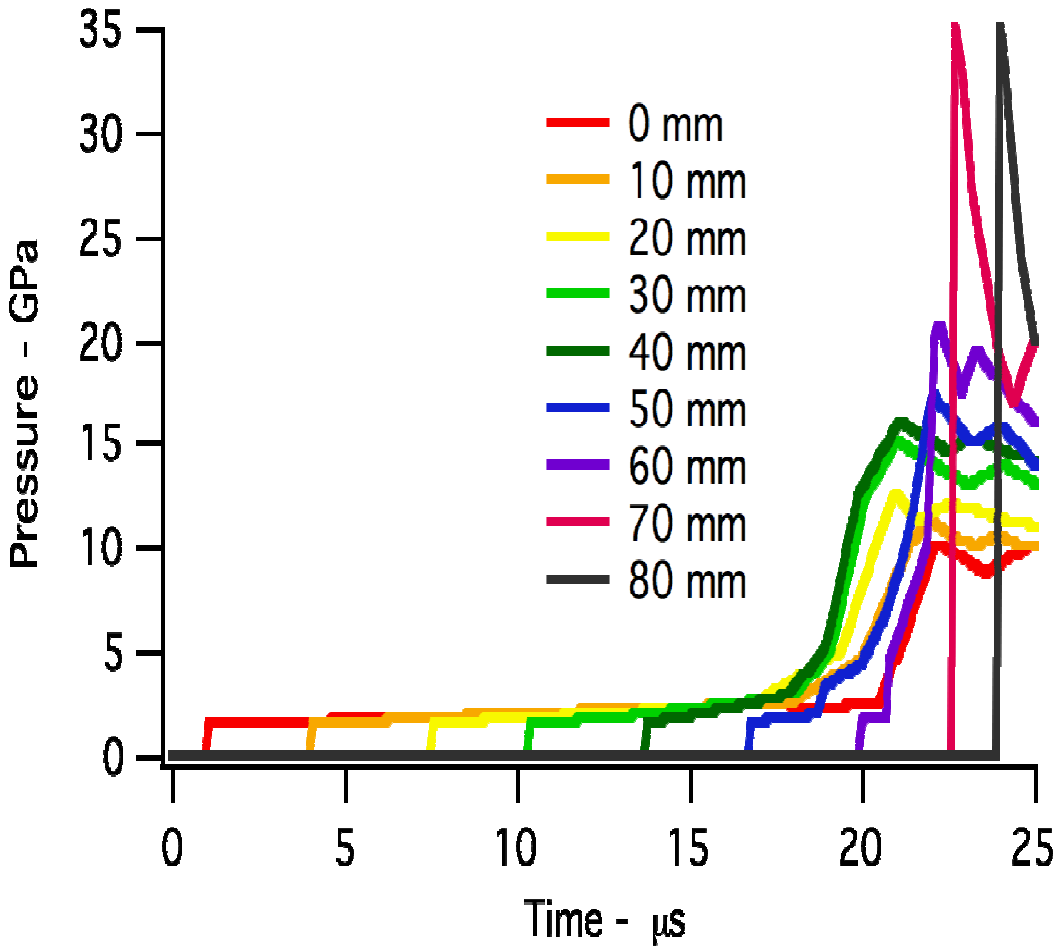

Figure 15. Calculated pressure histories for LX-07 shocked to 1.65 GPa

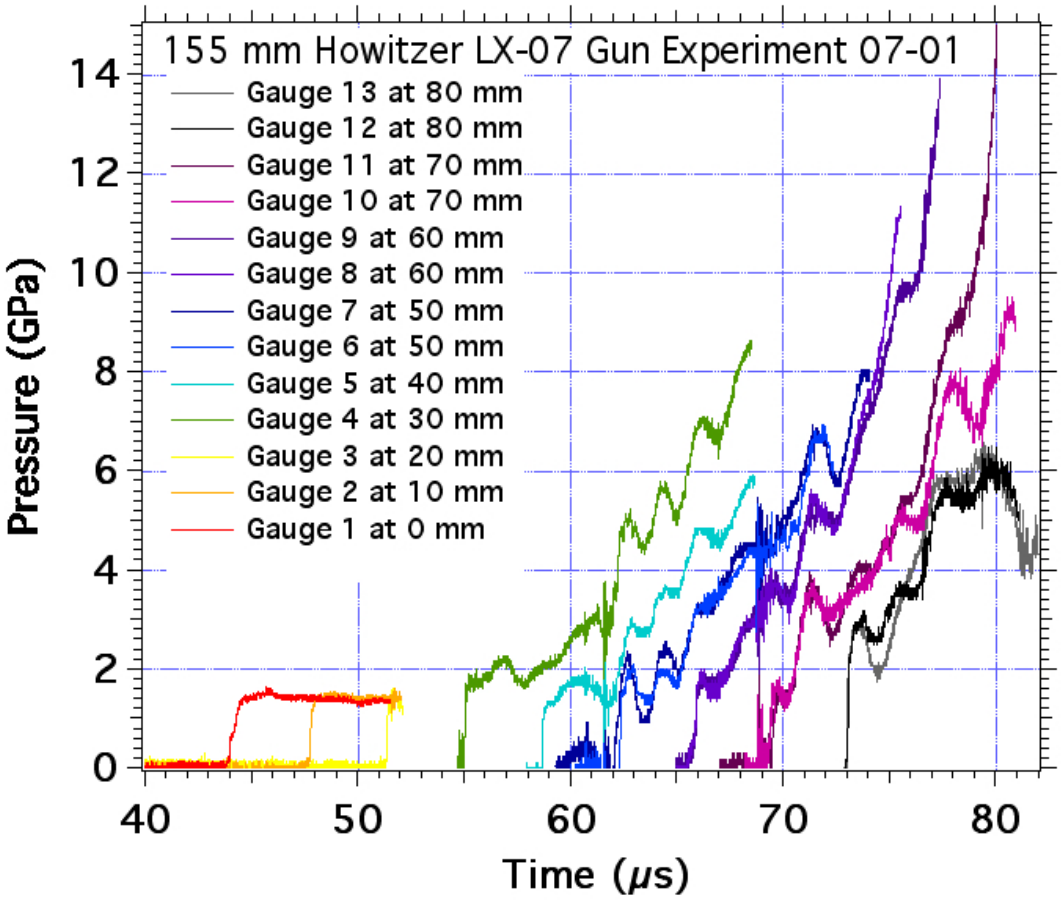

Figure 16. Experimental pressure histories for LX07 shocked to 1.55 GPa

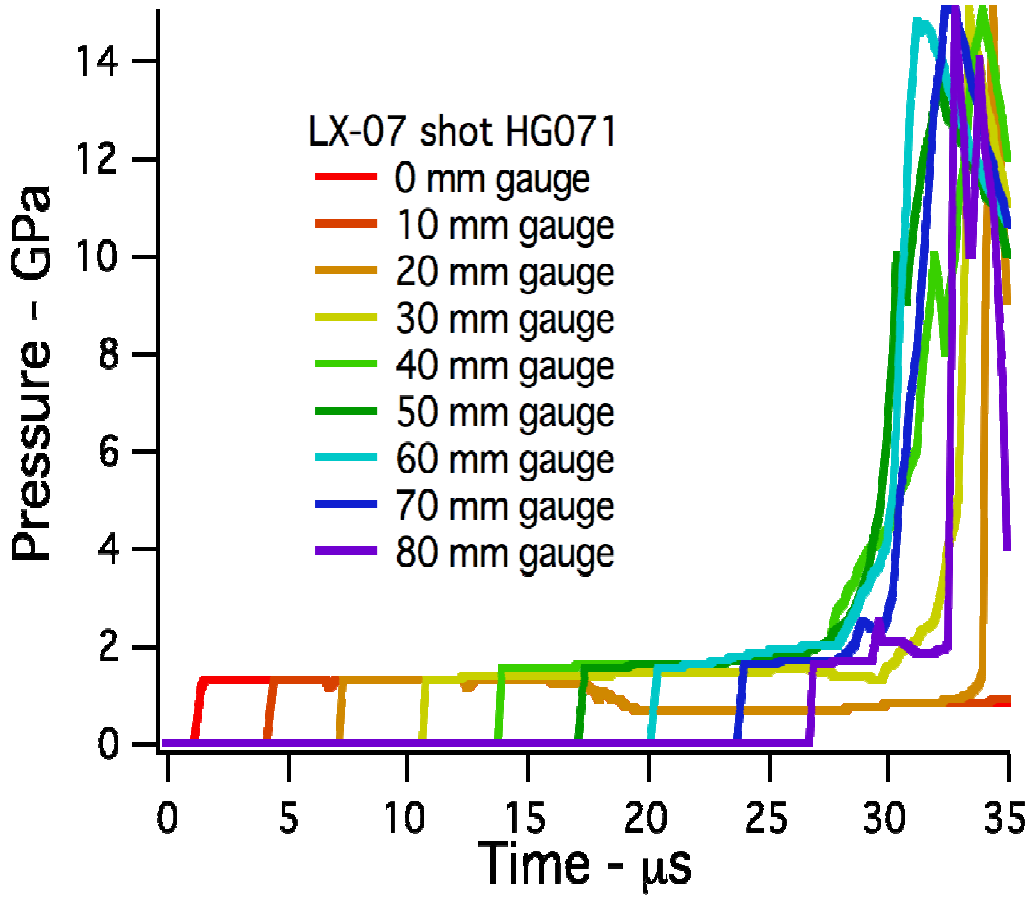

Figure 17. Calculated pressure histories for LX-07 shocked to 1.55 GPa

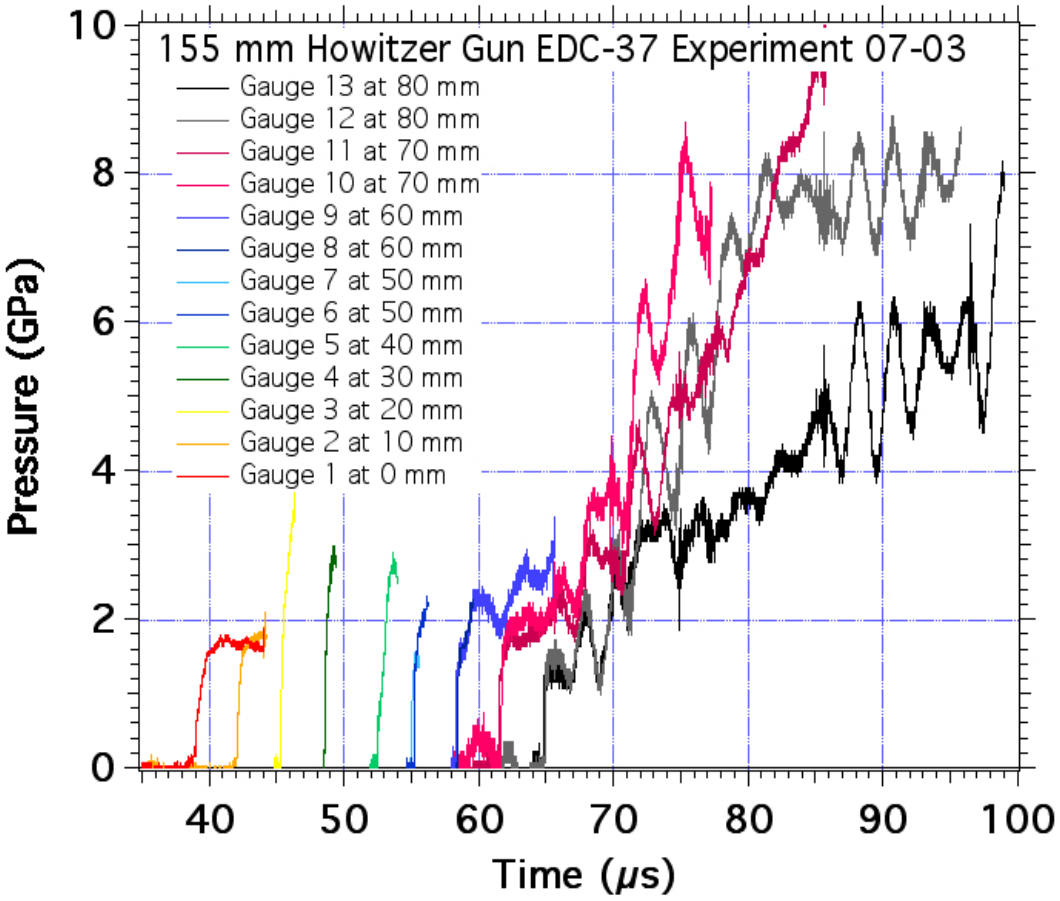

Figure 18. Experimental pressure histories for EDC37 shocked to 1.7 GPa

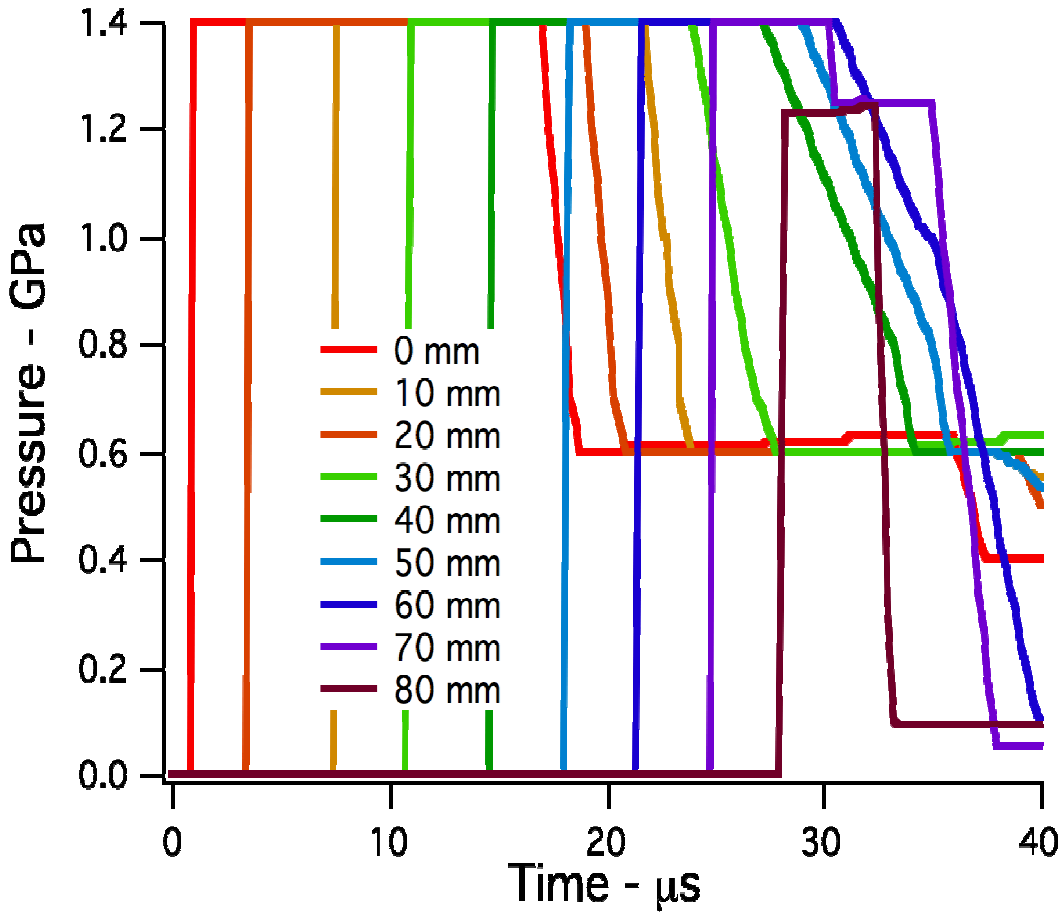

Figure 19. Calculated pressure histories for EDC37 shocked to 1.7 GPa

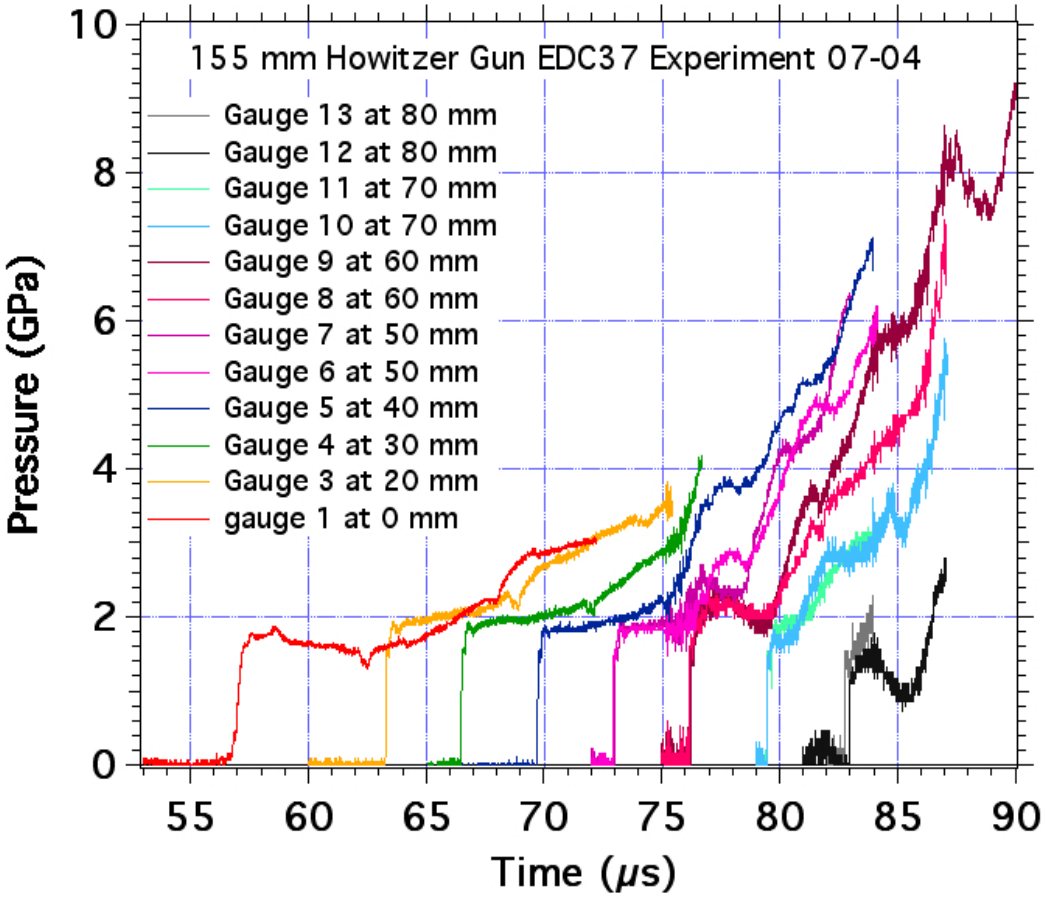

Figure 20. Experimental pressure histories for EDC37 shocked to 1.9 GPa

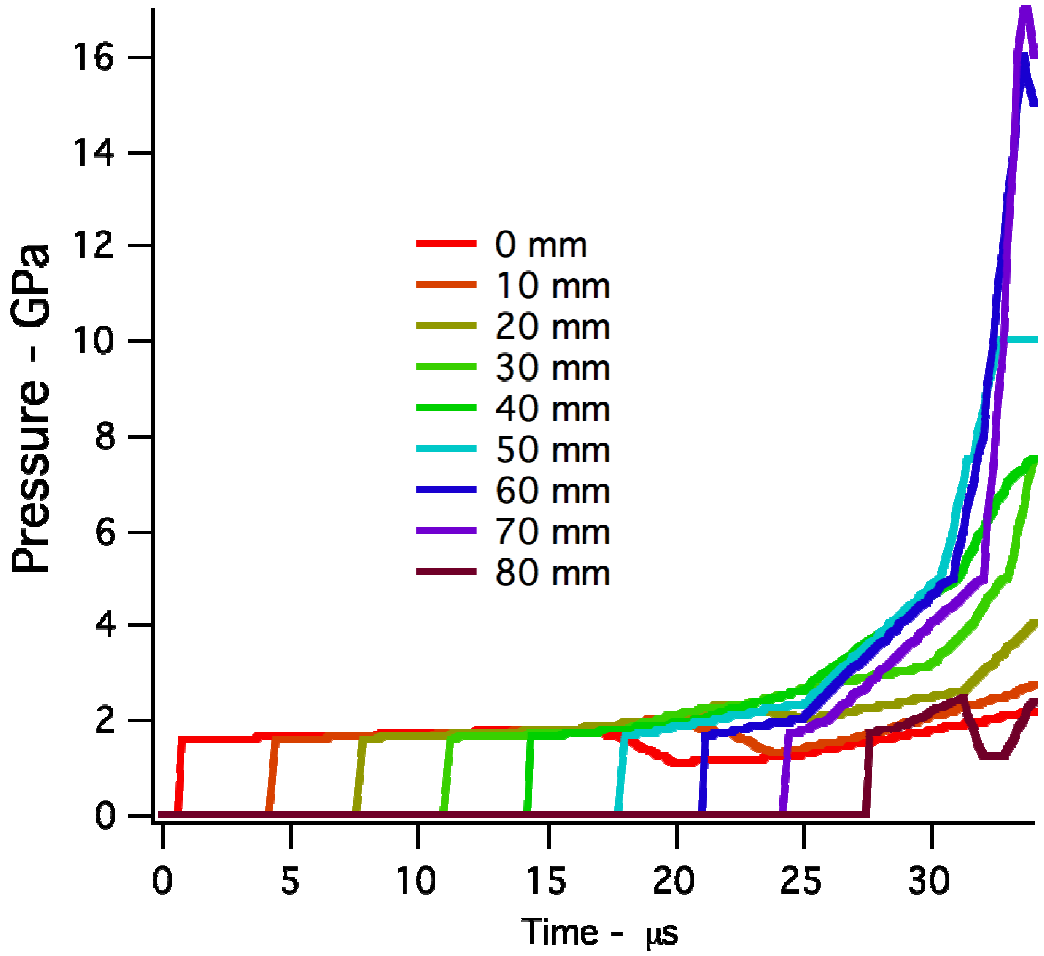

Figure 21. Calculated pressure histories for EDC37 shocked to 1.9 GPa

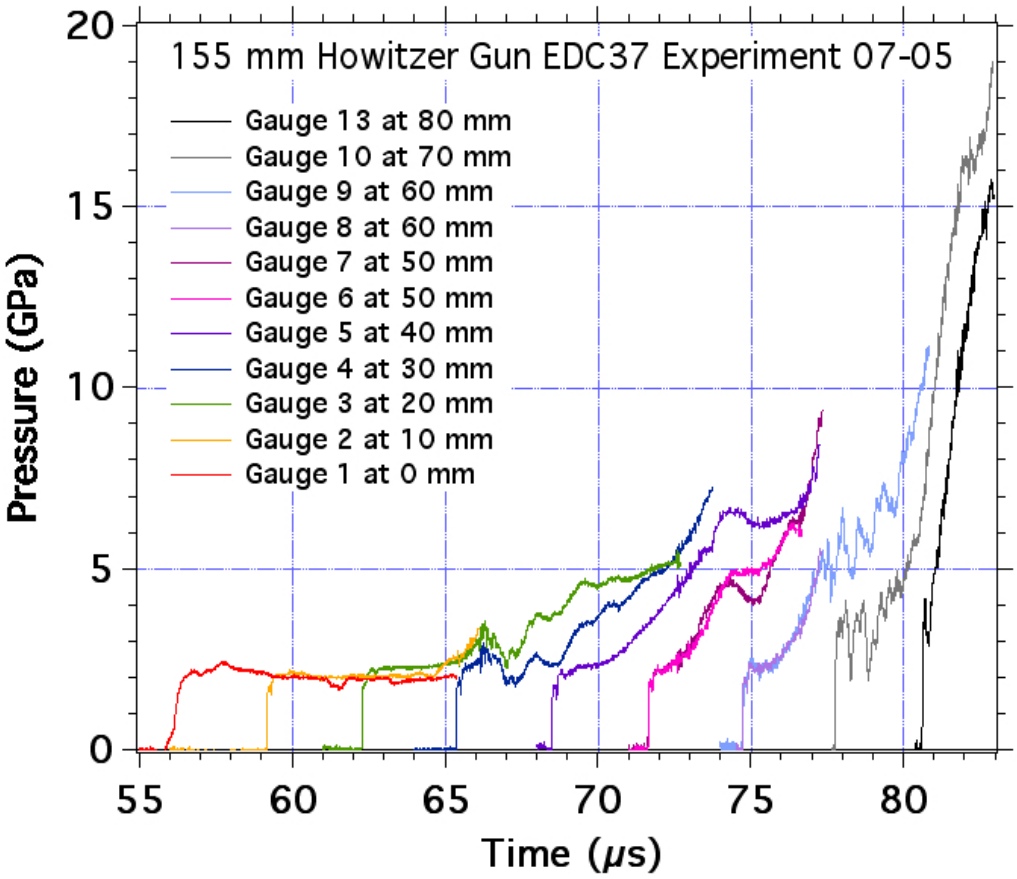

Figure 22. Experimental pressure histories for EDC37 shocked to 2.1 GPa

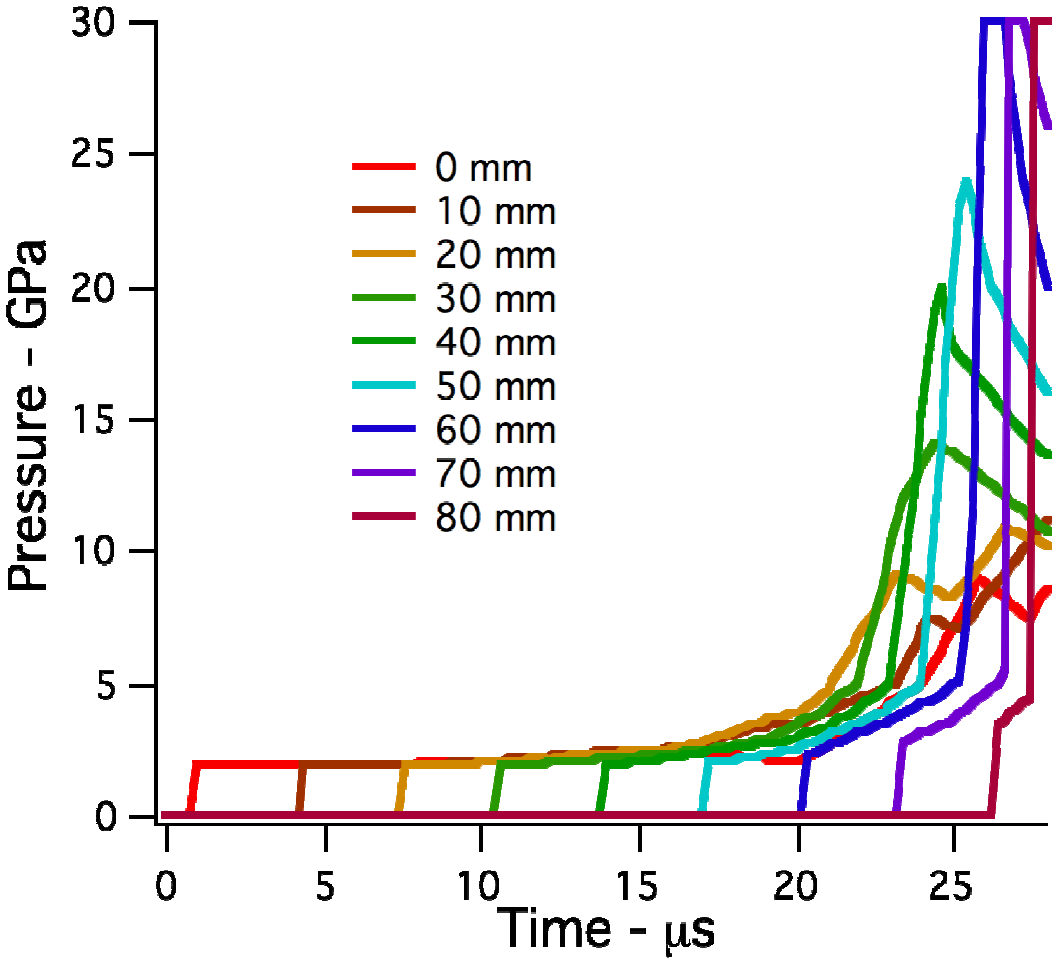

Figure 23. Calculated pressure histories for EDC37 shocked to 2.1 GPa

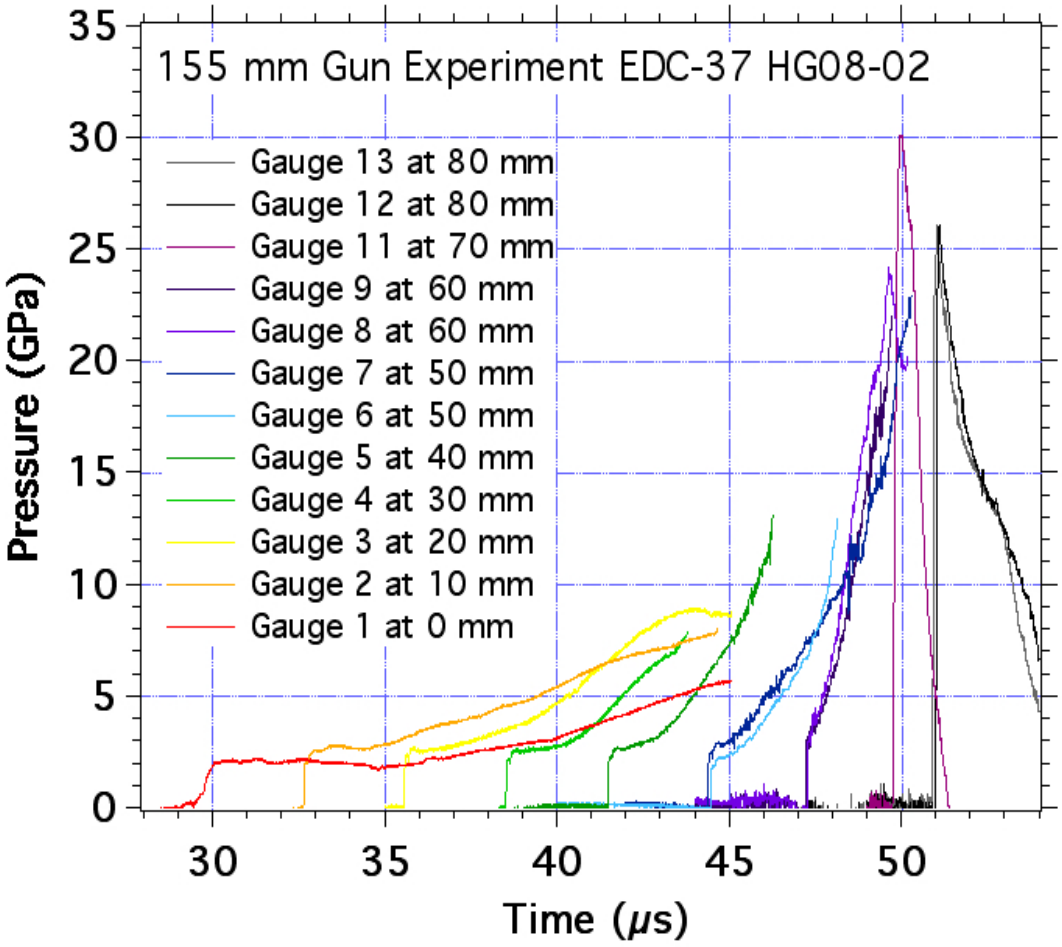

Figure 24. Experimental pressure histories for EDC37 shocked to 2.4 GPa

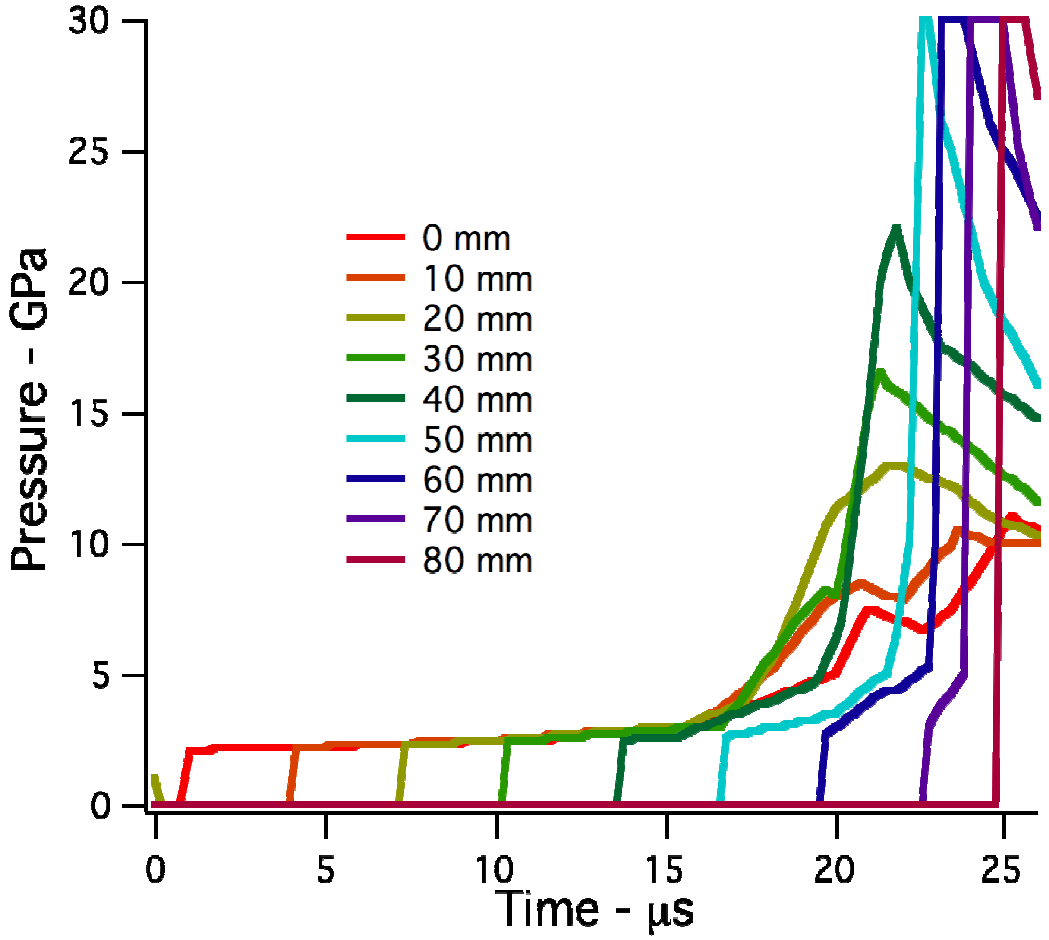

Figure 25. Calculated pressure histories for EDC37 shocked to 2.4 GPa

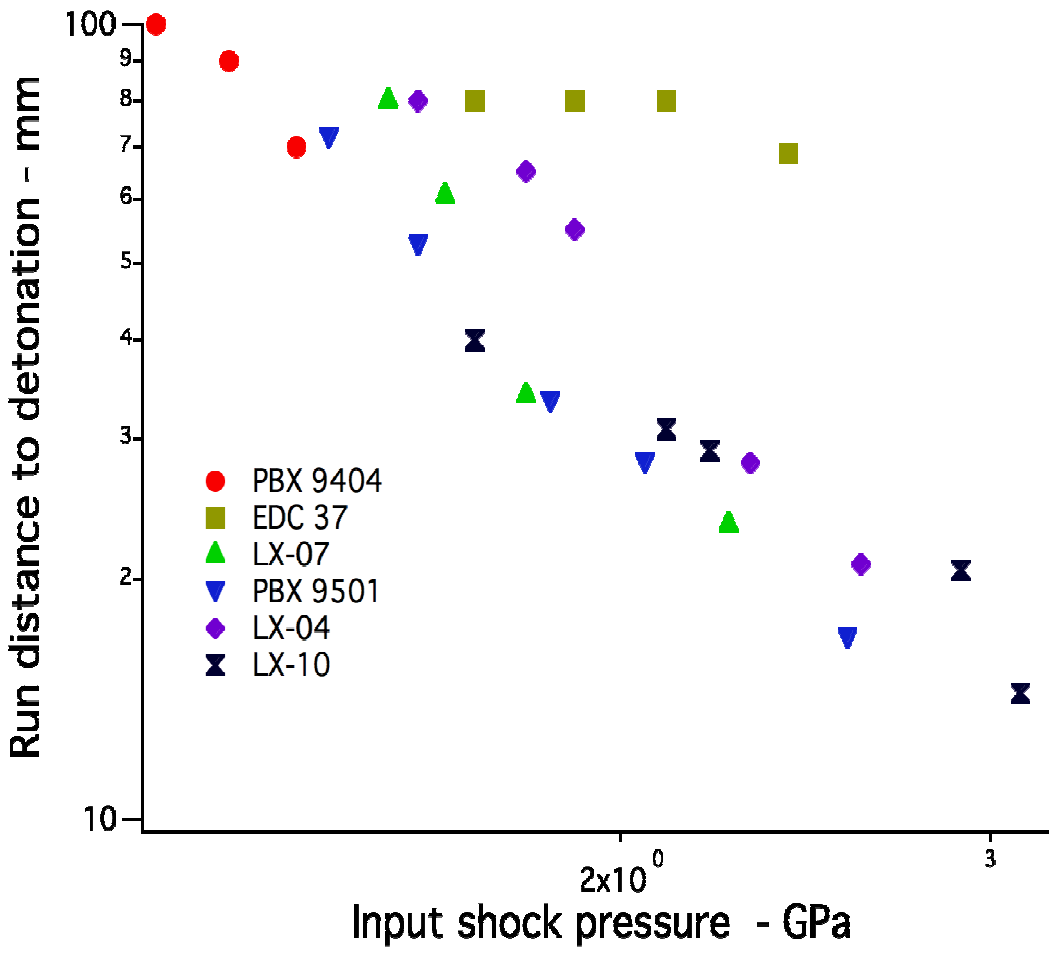

Figure 26. Low shock pressure run distances versus shock pressure for the six HMX PBX's